KC Mills*, L Yuan, Z Li, GH Zhang and KC Chou

A Review of the Factors Affecting the Thermophysical Properties of Silicate Slags

Abstract: This paper is dedicated to the memory of the of Prof. Masanori Iwase and his life and work. The factors which affect the thermo-physical properties of silicate and aluminno-silicate slags are reviewed. These include (i) the polymerisation of the silicate network (ii) various cation effects and (iii) temperature. Of these, the degree of polymerisation of the silicate network (expressed here through the parameter Q (= 4-NBO/T)) is the most important and the viscosity (η), electrical resistivity and thermal conductivity all increase as Q increases. Various ways in which different cations affect the properties are considered for each individual property *viz*. the *-M-O bond strength* affects (i) liquidus temperature (ii) activity coefficient of SiO_2 and (iii) thermal expansion coefficient and whereas both the *size and number of available cations* affect the electrical conductivity and resistivity.

The following observations were made:

i. There is less scatter in property data for liquid slags at a specific temperature than that for the liquidus temperature.
ii. The relation between Arrhenius parameters, ln A and B for viscosity and electrical resistivity is non-linear.
iii. The magnitude of the thermal conductivity (k) in solid slags is related to the rigidity of silicate network and the rapid decrease in k with increasing temperature occurs at a temperature where the viscosity reaches $\eta = 10^6$ dPas.
iv. The introduction of Al_2O_3 into the silicate chain results in significant changes to the properties

The ways in which the various properties can be calculated from chemical composition are outlined.

Keywords: slag properties, silicate-structure, cation-effects, property-estimation

PACS® (2010). 66.20-d, 72.15Cz, 68.03Cd, 65.60+a, 66.25+g

***Corresponding author: KC Mills:** Department of Materials, Imperial College, London, UK, E-mail: kcmills@talktalk.net
L Yuan: Manchester X-ray Imaging Facility, School of Materials, The University of Manchester, Oxford Rd., M13 9PL, UK
Z Li: Tata Steel Technology Centre, Rotherham, UK
GH Zhang: Metallurgical and Ecological Engineering School, University of Science and Technology, Beijing 100083, China
KC Chou: Metallurgical and Ecological Engineering School, University of Science and Technology, Beijing 100083, China

1 Introduction

This paper is dedicated to the memory of Prof Masanori Iwase and to his life and work.

Mathematical modelling has become essential to materials processing in the modern world. Before any prospective process is established it is necessary to establish models of:

i. The *thermodynamics* of the proposed process to establish its viability.
ii. The *kinetics* of the process to determine the production rate.
iii. The *mass, heat and fluid flow* to optimise process control and product quality.
iv. The *environmental impact* of the process.
v. The *economic viability* of the proposed process.

Prof. Masanori Iwase made significant contributions to our knowledge of the thermodynamics and kinetics of processes.

Slags play important roles in many processes, such as in metals processing, coal gasification, continuous casting. Their importance is summarised by the old adage used by steelmaking operators "*Look after the slag and the metal will look after itself*". The properties of slags are important in minimising problems in process control and are needed as input data in mathematical models of processes. The continuous casting of steel is a good example of the importance of slag properties; the molten slag infiltrates between the solid steel shell and the copper mould and forms a slag film consisting of a liquid layer and a solid layer [1]. The thickness of the liquid layer and the slag viscosity control the lubrication supplied to the shell and the thickness of solid layer controls the heat extraction from the shell which must be maintained at the optimum level to minimise cracks and breakouts [1]. Thus the *viscosity* and the *solidification temperature*

of the slag (which determines the thicknesses of liquid and solid layers) are the key slag properties, for continuous casting.

Mathematical modelling of processes has developed to the stage where it can be used to minimise process control problems and product quality issues. For instance, mathematical models of the continuous casting process provide insight into the mechanisms responsible for defect formation such as oscillation mark formation and slag entrapment [2, 3]. However, slag compositions tend to vary and thus their physical properties vary. The need for physical property data for slags is enormous and their measurement is time-consuming and requires considerable expertise. Consequently, there has been considerable effort to develop models to estimate slag properties from chemical composition since this is available on a routine basis. A large number of models have been published for calculating some properties (*eg*. viscosity) but there are few (or none) available for properties like thermal and electrical conductivities.

The objectives of the present study were:

i. to review the various factors affecting individual thermo-physical properties
ii. to comment on some routines used in the estimation of thermo-physical properties.
iii. To provide outlines of methods to calculate the thermo-physical property values for a wide range of silicate slags.

2 Methods

A large database of thermo-physical property measurements for slags has been established. This database was used to (i) analyse the factors affecting individual properties and (ii) to derive equations to represent the property in terms of the identified factors. These equations were derived from "*best fit*" constants for the various identified constants. Nonlinear models have to be used due to the complexity of the data fittings. An algorithm using the optimization toolbox in Matlab was used to fit the nonlinear models to data based on the method of least squares. Because of the nature of the approximation process, no algorithm is universal for all nonlinear models, data sets, and starting points. The final fitted constants are obtained by experimenting with different initial points in order to minimize the error distributions.

The sources of measurement values in the database for each individual property are given below in Section 3.

3 Factors affecting physical properties of slags

The thermo-physical properties of silicate slags are affected by (i) the silicate structure/network and (ii) the nature of the cations forming Metal-O (M-O) bonds and (iii) Temperature.

3.1 Effect of silicate structure

Pure SiO_2 consists of a 3D network in which each Si^{4+} is surrounded by 4 O^- ions which are arranged in the form of a tetrahedron and each O^- is bonded to two Si^{4+} ions. Thus SiO_2 is considered to be a *network-former* and the bonding is often denoted as "*IV coordination*" [4–6] and is covalent in nature. When cations, such as Na^+, are added (in the form of Na_2O) to SiO_2 they break some of the Si^{4+}-O^- bonds and replace them with ionic Na^+-O^- bonds. Further addition of Na^+ ions results in progressively- more depolymerisation of the melt; the Na^+ cations are referred to as "*network breakers*". Thus silicate slags contain both covalent and ionic bonds and the thermophysical properties are very dependent upon the level of polymerisation in the slag. The different types of bonds are classified in terms of the O bonds formed, namely, (i) *Bridging O's* (*eg*. Si-O) denoted both as BO and O^o (ii) *Non-bridging O's* denoted NBO or O^- and (iii) *Free-O's* (*ie*. bonded to cations and not to Si) denoted as O^{2-}.

When Al_2O_3 is added to silicate slags the Al^{3+} ions can be absorbed into the silicate structure. However, a Na^+ ion must be sited near the Al^{3+} to provide electrical charge balance (*ie*. forms ($NaAl^{4+}$)) [4–6]. It is considered that a Na^+ ion acting on charge-balancing duty can not act as a network breaker. Thus Al_2O_3 additions act principally as *network formers* but when large amounts of Al_2O_3 are added the Al^{3+} ions can also act as *network breakers* (*i.e*. exhibit *VI – fold coordination*) and for this reason Al_2O_3 is often referred to as an "*amphoteric*".

It might be anticipated that Fe_2O_3 and Cr_2O_3 would act like Al_2O_3 but there are indications that Fe_2O_3 acts as both *network breaker* and *network former* [7, 8]. It might also be expected that TiO_2 would fit readily into the silicate chain but viscosity data [9–13] indicate that TiO_2 additions reduce the viscosity which suggests that Ti^{4+} ions are acting as *network breakers*. Recent work [14–16] has indicated that when Fluorine is added to a silicate melt the F^- ions bond with Ca^{2+} ions to form CaF_2 which thereupon has little influence on the physical properties. This has led some workers to suggest that F^- additions promote polymerisation of the melt. However, in practice, any such

changes would be offset by the large decrease in liquidus temperature (T_{liq}) which results from fluorine additions.

It is important to have a parameter to represent the structure of the silicate slag. Several parameters have been used and are outlined below:

3.1.1 Basicity

Various basicity indices (eg. $\%CaO/\%SiO_2$) have been used to represent slag structure in the calculation of viscosities [17]. The major problem lies in dealing with oxides which can act as both a *networker-former* and *network-breaker* (eg. Fe_2O_3, Al_2O_3).

3.1.2 NBO/T and Q

The ratio of (Non-bridging O/Tetragonal O) ratio, which is denoted (NBO/T) is a *measure of the de-polymerisation* of the melt [4–6]. The (NBO/T) ratio is usually corrected to allow for cations acting on charge-balancing duties and it can also be corrected for the fraction of Fe_2O_3 acting as a network-breaker (f_{nb}) [8]. For a $CaO + Na_2O + Al_2O_3 + SiO_2$ slag the NBO/T ratio is given by Equation 1 where X is the mole fraction

$$(NBO/T) = 2(X_{CaO} + X_{Na_2O} - X_{Al_2O_3})/(X_{SiO_2} + 2X_{Al_2O_3}) \quad (1)$$

We prefer the parameter, Q, which is a *measure of the polymerisation* of the melt and which can be calculated from (NBO/T) using Equation 2.

$$Q = 4 - (NBO/T) \quad (2)$$

3.1.3 Optical basicity (Λ)

The major problem when using (NBO/T) or Q lies in the fact that it does not differentiate between different cations *eg*. Na^+ or Ca^{2+}. The *optical basicity* was introduced to partially resolve this problem [18–20]. The *optical basicity* (Λ) is a measure of the electron donor properties of different ions [21, 22]. It was also used as a measure of the depolymerisation of the melt [9, 10] and can be calculated by Equation 3 where m is the number of O atoms *eg*. 1 for CaO and 2 for SiO_2 and Λ_1 is the optical basicity value for oxide 1.

$$\Lambda = \Sigma(X_1m_1\Lambda_1 + X_2m_2\Lambda_2 + X_3m_3\Lambda_3 + \cdots)/\Sigma(X_1m_1 + X_2m_2 + X_3m_3 + \cdots) \quad (3)$$

The composition can be corrected to allow for the cations on charge-balancing duties [18]. The principal disadvantage to the use of optical basicities results from:

i. Uncertainties in the Λ values for some components *eg*. transition metal oxides (*eg*. FeO) and CaF_2.
ii. The optical basicity is a reasonable measure of the M-O bond strength [18] but does not differentiate between the size of cations which is important in electrical resistivity.

3.1.4 Concentrations of O^o; O^- and O^{2-}

The structure can be represented in terms of the concentrations in the slag of *bridging* O's (O^o) *non-bridging O's* (O^-) and *free O's* (O^{2-}). The principal limitation to this approach has been that it requires a mathematical model [23–25] to determine these concentrations. However, recently a method has been developed to calculate these concentrations without the aid of a mathematical model [26–29] and this would appear to be exceedingly useful in predicting properties since it can differentiate between Si-O and Al-O bonds and their effects on specific properties.

3.2 Effect of cations

A list of the different ways in which the cation can affect the properties is given below. The following list is not exclusive and other mechanisms (eg. transfer of electrons between Fe^{2+} and Fe^{3+}) may also play a part.

3.2.1 Metal-Oxygen bond strength

The strength of the bond between a non-bridging oxygen and a cation (depicted in Figure 1) is usually represented by the parameter (z/r^2) where z is the charge and r is the cation radius. Other workers [30] have used bond strength values but these are not available for all slag components. Consequently, if the strength of this M-O bond is a key parameter affecting the property, for slags with equivalent compositions, property values will be in the order Mg > Ca > Sr > Ba > Li > Na > K ((see Section 5)) or in the reverse order. The value of r and z/r^2 are given in Table 1. It should be noted that some properties, such as thermal expansion, the hierarchy of property values differ slightly from the hierarchy of z/r^2 values given in Table 1 (especially with Li, Ba and Sr) and this may indicate a limitation in using (z/r^2) as a measure of M-O bond strength.

Fig. 1: Schematic diagram showing relative strengths (denoted by thickness of bond) of M^{+}-O^{-} bonds for Li^{+}, Na^{+} and K^{+}.

	Li_2O	Na_2O	K_2O	MgO	CaO	SrO	BaO	FeO	MnO
$10^{10}r$ (m)	0.76	1.02	1.38	0.72	1.0	1.18	1.35	0.74*	0.80*
z/r^2	1.73	0.96	0.53	3.85	2.0	1.43	1.1	3.65	3.13
$(r_M/r_{Ca})^3$	0.44	1.06	2.63	0.373	1.0	1.64	2.46	0.405	0.512

Table 1: Values of the cation radius (r) the relative values of the parameter (z/r^2) and $(r_M/r_{Ca})^3$ [31]; * indicates from reference [32].

3.2.2 Nature of metal-O bond strength

Although the bond between a non-bridging oxygen (NBO) and a cation is largely ionic in nature it also contains some covalent contribution. Recently, Zhang et al [26] showed that hierarchy of viscosities for equivalent compositions of MO-SiO_2 was distorted by the higher level of covalent contributions in Fe^{2+} and, to a less extent, in Mn^{2+}-O bonds.

3.2.3 Bridging of chains by cations

If a Ca^{2+} ion acts as either as a *network breaker* or as a *charge balancer* for an Al^{3+} ion, in order to utilize its double charge, it must form a link to a second non-bridging oxygen (O^{-}) or another Al^{3+}, respectively. This link tends to restrict the movement of the silicate unit and hence tends to increase the viscosity or decrease the electrical conductivity. This is not the case for Na^{+} ions so the viscosities of silicates containing Group I oxides (M_2O) tend to be lower than those containing Group 2 oxides (MO). Thus any Fe^{3+} acting as a network breaker or as a charge balancer would have to involve 3 silicate chains which would be expected to cause even more hindrance to movement than a Ca^{2+}. "*Bridging*" is depicted in Figure 2.

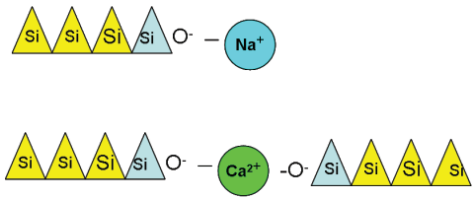

Fig. 2: Schematic representation of "*bridging*" with Ca^{2+} ions *cf* absence of bridging for Na^{+} ions.

3.2.4 Size of cations

Viscosities are a measure of the resistance to the movement of one silicate unit over another. Thus it might be anticipated that large cations could possibly hinder this movement (depicted in Figure 3a). Electrical conductivity involves the transport of cations through the silicate network. Thus it would be anticipated that smaller cations will be more successful than bigger cations in passing through the network (Figure 3b) and consequently, will have a higher electrical conductivity. This is referred to here as the "*hindrance effect*". In these cases, the hierarchy in resistance to movement will correlate with values of (r^3).

3.2.5 Number of cations

For Na_2O-SiO_2 and CaO-SiO_2 slags with equivalent composition (*ie.* same X_{SiO_2}) there are twice as many Na^{+} ions as Ca^{2+} ions; the number of available cations (n) is important

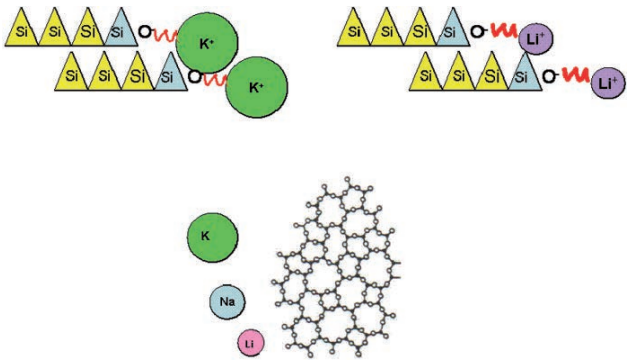

Fig. 3: Schematic diagram showing hindrance caused by large cations in (top)- viscosity and (bottom) electrical conductivity.

in properties like electrical conductivity and diffusion. However, it would be anticipated that those cations performing charge-balancing duties will not be available for charge-transport.

3.2.6 Mixed alkali effect

For systems such as K_2O-Li_2O-SiO_2 the replacement of Li^+ ions by K^+ results in a significant decrease in values of electrical conductivity, ionic diffusivity and T_g. This is known as the *mixed cation effect*. It occurs when there is a significant difference in the sizes of the two ions which results in defects when the mobile ions enter foreign sites [33].

The effect of the above on the properties can be deduced by comparing values of the property values for slags with similar compositions but containing different cations. The hierarchy of the property values at a reference temperature can be used to determine, for instance, whether there is a dependence on MO-bond strength (z/r^2) or cation size (r^3). Many workers have used the liquidus temperature (T_{liq}) as the reference temperature. Consider two slags, A and B, with T_{liq} values of 1400 and 1800 K, respectively. A comparison of the viscosities of A and B at say, 1900 K, would mean that the viscosity of A would decrease over a period of 500 K compared with only 100 K for B. This is denoted here as "*the T_{liq} effect*" and will be discussed in Section 4.3.

3.3 Effect of temperature

Slag properties are very sensitive to temperature and this sensitivity increases with increasing polymerisation of the melt. Increasing temperature tends to loosen the silicate structure (akin to the de-polymerisation caused by cations). Thus the effect of increasing temperature on various properties can be predicted by its effect on de-polymerisation (namely, decreasing viscosity, electrical resistivity and thermal conductivity).

3.3.1 Solid slags

Solid slags can exist as *glassy* or *crystalline* phases or, in some cases as mixtures of glass and crystalline phases. The form of the slag is dependent upon (i) composition (glasses are promoted by high Q value) (ii) the thermal history of the sample.

Glassy slags undergo a transition from glass → supercooled liquid (*scl*) at the glass transition temperature (T_g). This transition is accompanied by changes in physical properties at T_g *eg*. a "*step-like*" increase in C_p and a 3-fold increase in thermal expansion coefficient, α, above T_g. (Figures 4a and b, respectively). The viscosity of the slag in the form of a supercooled liquid is taken to be $\eta = 10^{13.4}$ dPas at T_g. These enhanced C_p and α values are maintained throughout the *scl* region between T_g and T_{liq}. The transition of *scl* → liquid is accompanied by zero, or low, values for the enthalpy of fusion (ΔH^{fus}) and ΔV^{fus}. Values of T_g can be calculated [34] using Equation 4 which was obtained from a "*best fit*" of composition and T_g values (derived from (i) experimental T_g data obtained from C_p or thermal expansion studies and (ii) temperatures where $\eta = 10^{13.4}$ dPas using the Fluegel model [35]). Note Equation 4 is preferred to a previously-published equation for calculating T_g [36].

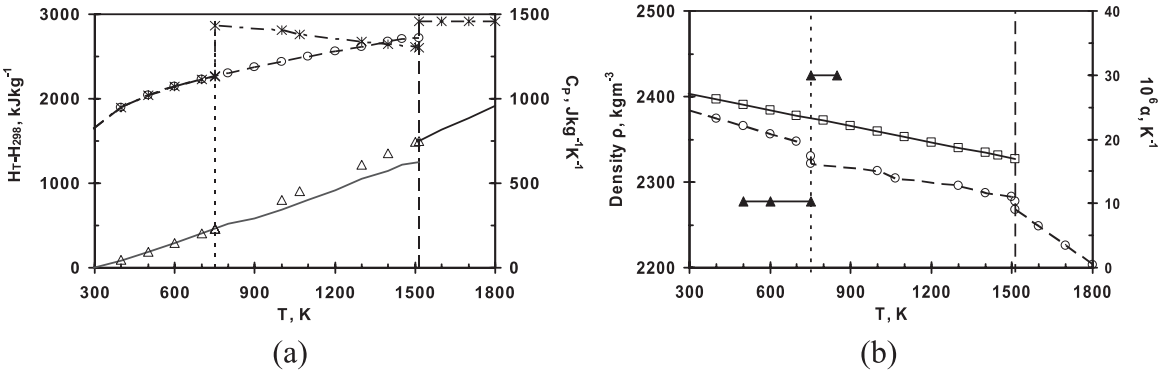

Fig. 4: Schematic diagrams showing the effects of the glass transition on (a) C_p and enthalpy (H_T-H_{298}) C_p: -.-. , and X = *scl*; o and solid line = glass and crystalline phase and (H_T-H_{298}): solid line = glass, crystalline and liquid phases; Δ = *scl*; and (b) density and thermal expansion coefficient, α; Density □ = crystalline phase; glass and *scl* and liquid phases; α; ▲ = glass and *scl* phases.

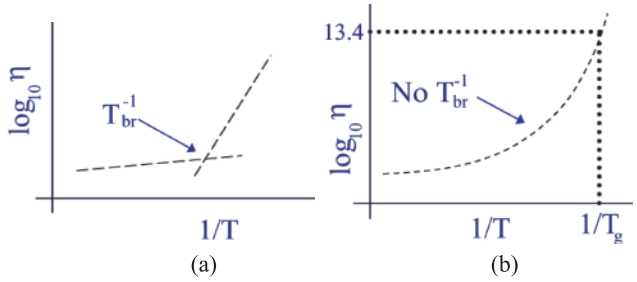

Fig. 5: Plots of $\log_{10}$ viscosity as functions for reciprocal temperature (K^{-1}) for (a) a slag where crystallites are precipitated (Q = 2) and (b) glassy slag forming a scl (Q > 2.5).

$$\begin{aligned} T_g(K) = {} & 910.1 - 102.2X_{SiO_2} + 414.5X_{CaO} + 15.1X_{Al_2O_3} \\ & - 388.5X_{Na_2O} - 394.9X_{Li_2O} - 342.4X_{K_2O} \\ & - 35.4X_{MgO} - 3541X_{CaF_2} + 547X_{MnO} + 1634X_{FeO} \\ & - 53.5X_{SrO} - 318.4X_{BaO} + 96.4X_{TiO_2} + 4.14X_{ZrO_2} \\ & - 1782X_{Fe_2O_3} \end{aligned} \quad (4)$$

In contrast, C_p and α values for the crystalline phase increase smoothly with increasing temperature up to T_{liq}; at T_{liq} there is an abrupt increase in the enthalpy and volume of the slags (*ie*. ΔH^{fus}, ΔV^{fus}). Figure 4 shows the enthalpy (H_T-H_{298}) and density (ρ) as a function of temperature.

3.3.2 Liquid slags

When a molten slag is cooled below T_{liq} it forms either crystallites or a supercooled liquid. If viscosities are measured in a cooling cycle, when solid particles (crystallites) are formed (Figure 5a) there is a sharp increase in viscosity. In contrast, when a liquid slag transforms to a *scl* it is accompanied by a smooth increase in viscosity (Figure 5b).

4 Factors affecting individual properties

In this section we examine the effects of silicate structure, cations and temperature on individual physical properties.

4.1 Liquidus temperature (T_{liq})

The liquidus temperatures of binary silicate slags are affected by the M-O bond strength with T_{liq} values decreasing as (z/r^2) decreases [18, 34]. However, T_{liq} values are also affected by the nature of the phase formed. Thermodynamic models [37–39] can provide reliable values for T_{liq} because they contain information for the various phases formed. Values of T_{liq} derived from best fits of T_{liq}-composition data, such as that shown in Equation 5, are prone to uncertainties of ±100 K, or more [36].

$$\begin{aligned} T_{liq}(K) = {} & 958 + 656.9X_{SiO_2} + 1040.7X_{CaO} + 1343X_{Al_2O_3} \\ & + 137X_{Na_2O} + 408.7X_{Li_2O} - 668X_{K_2O} + 1091X_{MgO} \\ & - 532X_{CaF_2} + 761X_{MnO} + 522X_{FeO} + 1022X_{CrO} \\ & + 2198X_{Cr_2O_3} + 1768X_{SrO} + 1207X_{BaO} + 844X_{TiO_2} \\ & + 2234X_{ZrO_2} + 794X_{Fe_2O_3} - 12.6X_{B_2O_3} \end{aligned} \quad (5)$$

4.2 Thermodynamic properties

4.2.1 Activity coefficient of SiO_2 ($f^*_{SiO_2}$)

The activity coefficient of SiO_2 ($f^*_{SiO_2}$) is a measure of the ability of Si ions to escape; thus $f^*_{SiO_2}$ would be expected to decrease as the M-O bond strength increases (*ie*. increasing z/r^2). It can be seen from Figure 6 that the activity coefficient of SiO_2 ($f^*_{SiO_2}$) increases with decreasing (z/r^2) for any specific SiO_2 content (*ie*. Q value) for both MO-SiO_2 and M_2O-SiO_2 systems.

4.2.2 Heat capacity (C_p) enthalpy (H_T-H_{298})

The heat capacities of slags follow Kopp's Rule well and thus can be calculated using partial molar procedures ($C_p = \Sigma X_1 C_{p1} + X_2 C_{p2} + X_3 C_{p3} +$) where 1, 2, 3, represent the various slag constituents.

The heat capacity of glassy slags exhibits a "*step-like*" increase at T_g whereas crystalline slags continue their smooth dependence on temperature until fusion occurs (Figure 4a).

4.2.3 Entropy of fusion (ΔS^{fus})

It can be seen from Figure 6 that the entropy of fusion (ΔS^{fus}) of the *crystalline phase* shows the expected result, *ie*. that ΔS^{fus} increases with increasing (z/r^2) *ie*. increasing M^+-O^- bond strength [18]. It is considered here that ΔS^{fus} has a zero, or low, value for the transition, *scl* → liquid.

4.3 Viscosity (η)

Database: liquid [9–14, 40–45] Experimental uncertainty ±10–25% scl [35].

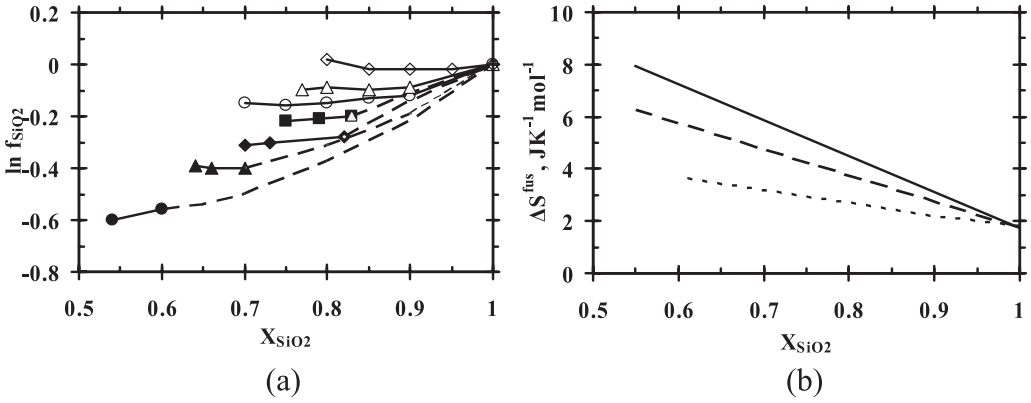

Fig. 6: The effect of mole fraction SiO_2 on (a) logarithm of activity coefficient of SiO_2 (ln $f^*_{SiO_2}$) as a function of mole fraction of SiO_2 for M_2O-SiO_2 and M_2O-SiO_2 slags [18]; ● = MgO; ▲ = CaO; ♦ = SrO; ■ = BaO; O = Li_2O; Δ = Na_2O; ◊ = K_2O; dashed lines = extrapolations and (b) entropy of fusion; solid line = LS; dashed line = NS; dotted line = KS [18, 34].

4.3.1 Factors affecting viscosity values of liquid slags

Temperature

The viscosities of silicate slags are dependent upon (i) the structure or degree of polymerisation of the melt (ii) cation effects and (iii) temperature.

It is customary to express the viscosities of liquid slags in the form of Arrhenius or Weymann equations (Equations 6 and 7, respectively) where A is a pre-exponential term and B (= E/8.314) where E is the activation energy.

$$\ln \eta = \ln A_A + (B_A/T) \quad (6)$$

$$\ln(\eta/T) = \ln A_W + (B_W/T) \quad (7)$$

The ln A and B values are derived from the intercept and slope, respectively, of plots of the terms on the left-hand-side against (1/T). Values of ln A tend to be scattered because (1/T) = 0 corresponds to infinite temperature and thus ln A is very sensitive to uncertainties in the slope (B). Consequently, data which includes values for temperatures where $T < T_{liq}$ (corresponding to either a *scl* or to a "mushy phase") can lead to errors in ln A. Consequently, some workers have derived ln A values by assuming ln A is a linear function of B [7]. However, recent work has shown (Figure 7a) that (i) the relation between ln A and B is non-linear and (ii) the B values for MO-silicate and M_2O-silicates fall on different curves [34].

The temperature dependence of the supercooled phase is usually expressed in the form of the Vogel-Fulcher-Tammann (VFT) equation where T_o is a variable (Figure 7b); this type of equation is denoted here by the subscript V.

$$\ln \eta = A_V + B_V/(T - T_o) \quad (8)$$

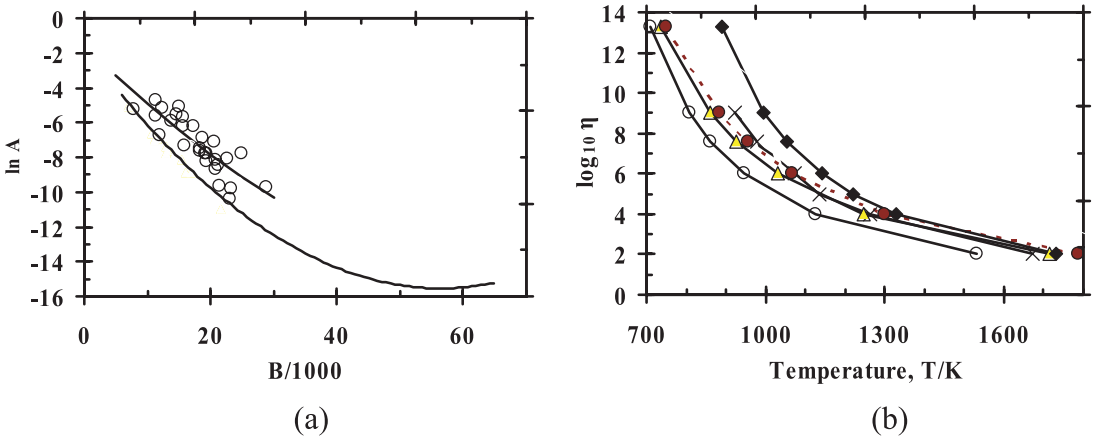

Fig. 7: The parameter, ln A_A as a function of the activation energy term, B_A, the upper curve and O = M_2O-silicates and lower curve = MO-silicates and (b) The temperature dependence of the viscosities of slags in the supercooled liquid phase; ♦ = 0.1Na_2O 0.2CaO 0.7SiO_2; x = 0.2Na_2O 0.1CaO 0.7SiO_2; ● = 0.2Na_2O-0.8SiO_2; Δ = 0.25Na_2O-0.75SiO_2; O = 0.333Na_2O-0.667SiO_2. [35]

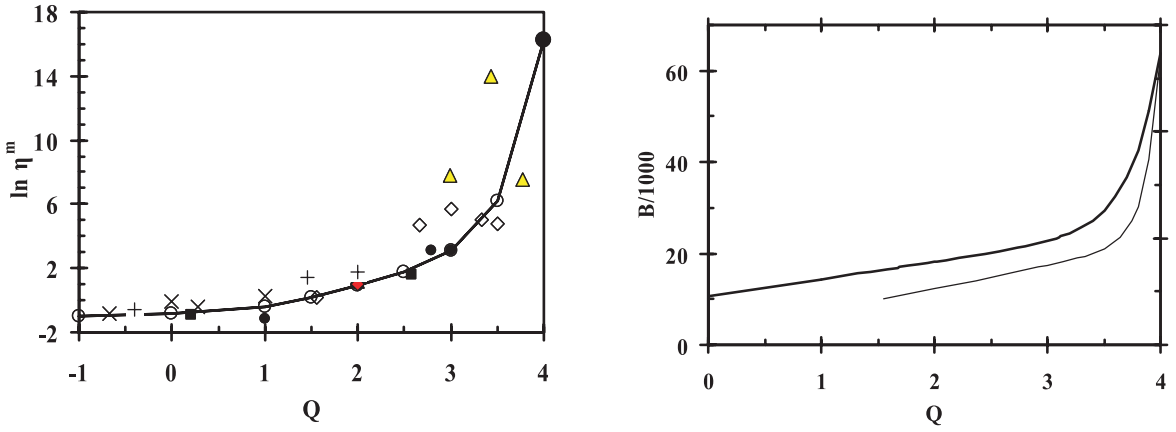

Fig. 8: (a) ln η^m as a function of the polymerisation parameter, Q; ◊ = LS; ○ = NS; Δ = KS; ■ = MS; ● = CS; ▲ = SrS; ♦ = BS; x = FS; + = MnS; • = SiO_2; line = suggested curve (b) the term (B_A) for viscous flow as a function of Q; upper curve = MO-SiO_2 and lower curve M_2O-SiO_2 systems [34].

Effect of silicate structure

The effect of the polymerisation parameter on both ln η^m (*ie*. the value at T_{liq}) and the activation energy term, B_A are shown in Figure 8. It can be seen that:

i. Both ln η^m and B_A are functions of Q and can be expressed in the form of Equation 9

$$\ln \eta^m \text{ (or } B_A) = y + c_1 \exp(Q/t_1) + c_2 \exp(Q/t_2) \quad (9)$$

ii. B_A values for MO-silicates and M_2O-silicates fall on different curves.

The T_{liq} effect

It was pointed out in Section 3.2 that it is customary to compare properties at the liquidus temperature. Inspection of Figure 8a shows that there is appreciable scatter in the M_2O-silicates data with K_2O-silicates (shown as Δ) exhibiting higher viscosities; this was initially attributed to the differences in cation size [34]. However it was realised that the M_2O-silicates exhibited a wide range in T_{liq} (1078–1743 K) thus it was decided to compare viscosities at a reference temperature (1773 K). The results, shown in Figure 9, indicate that:

i. the scatter in the ln $\eta_{1773\,K}$ data is significantly less than that in ln η^m and it would appear that the practice of comparing property values at T_{liq} is seriously flawed and it is preferable to carry out comparisons at a reference temperature.
ii. there is less scatter in ln η^m data for the MO-SiO_2 (which is probably due to the fact that T_{liq} are both higher and are closer together) but even here ln $\eta_{1900\,K}$ values show less scatter than ln η^m data (Figures 9c and d).
iii. the ln $R_{1900\,K}$ values for M_2O-SiO_2 systems lie on a slightly lower curve than that for MO-SiO_2 systems.

Effect of cations

It can be deduced from Figures 9 (b) and (d) that any cation effects on the viscosity are relatively small. The curve shown in Figure 9d was obtained through a best fit of ln $\eta_{1900\,K}$ data for both M_2O and MO-silicates (ln $\eta_{1900\,K}$ = $-2.161 + 0.8279 \exp(Q/1.794) + 2.19 \times 10^{-16}(Q/0.1036)$. Close inspection of the data in Figure 9d indicate that deviations from the ln $\eta_{1900\,K}$-Q curve:

i. exhibit a weak correlation with increasing cation size $(r_M/r_{Ca})^3$ ($\Delta \ln \eta_{1900\,K} = \{0.22\,(r_M/r_{Ca})^3\}$ or $\{0.72X_{MO+M_2O}\,(r_M/r_{Ca})^3\}$.
ii. tend to be negative for M_2O-silicates and positive for MO-silicates *ie*. M_2O silicates lie on a slightly lower curve than that for MO-silicates.

It can be seen from Figure 8b that the activation energy parameters, B_A, that for MO-SiO_2 and M_2O-SiO_2 systems fall on different curves which could be due to "*Bridging of chains*" by M^{2+} ions.

4.3.2 Effects of Al_2O_3, Fe_2O_3, Cr_2O_3, TiO_2, and CaF_2

Alumino-silicates

The absorption of Al_2O_3 into the silicate network (for a given Q value) results in decreases from the silicate values for both ln $\eta_{1900\,K}$ and the activation energy term, B_A (Figure 10). The value, Q = 4, pertains to pure SiO_2, but also to alumino-silicates in which $X_{MO+M_2O} = X_{Al_2O_3}$. It can be seen from Figure 10 that:

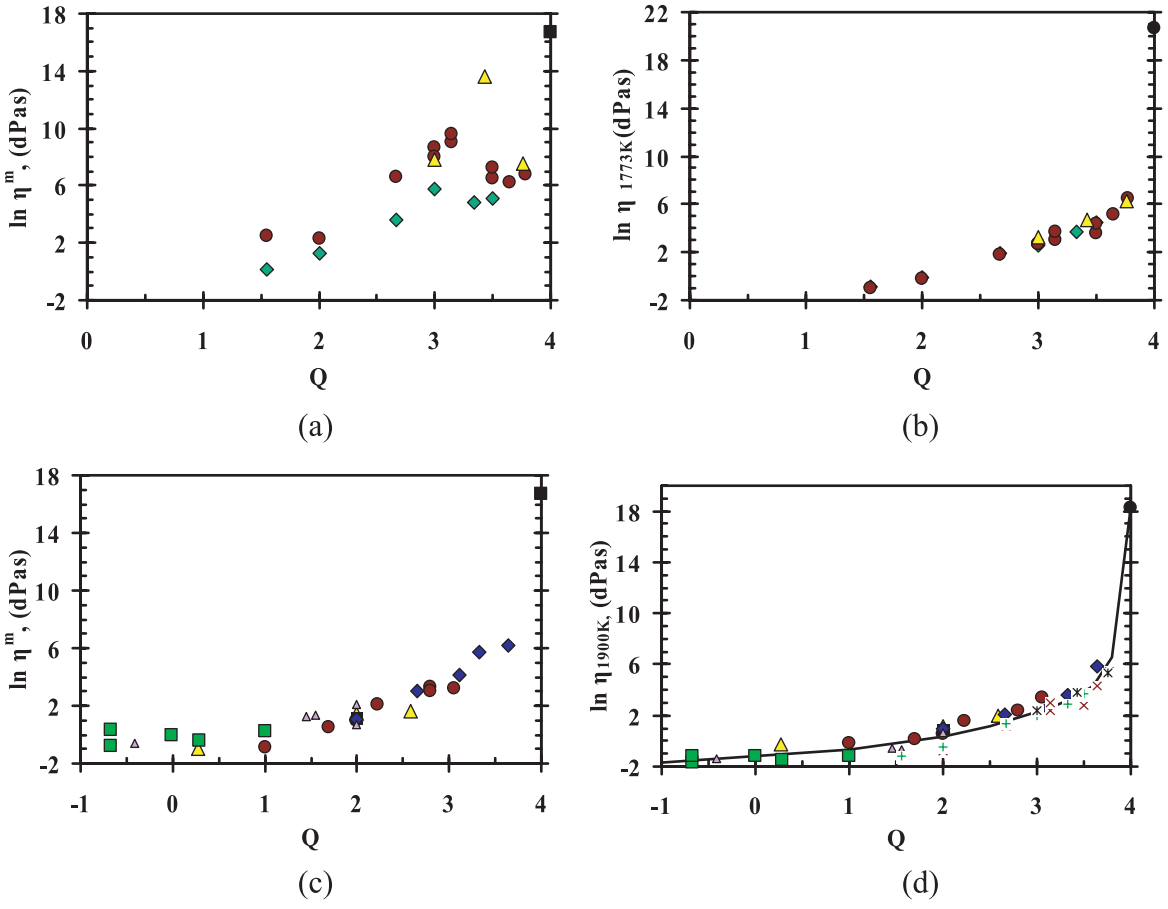

Fig. 9: Comparison of (a) ln η^m and (b) (a) ln $\eta_{1773\,K}$ for M_2O-SiO_2 systems; Δ = K_2O; ● = Na_2O; ♦ = Li_2O and ■ = SiO_2 and (c) ln η^m for MO-SiO_2 systems and (d) ln $\eta_{1900\,K}$ for both MO and M_2O-SiO_2 systems; ● = CS; ♦ = BS; ■ = SrS; Δ = MS; □ = FS; ▵ = MnS; + = LS; x = NS; * = KS; ■ = SiO_2; curve = best fit of data.

i. there is a wide spread in both ln η^m and B_A* (= B_A/1000) values for the alumino-silicates and it was observed that both ln η^m and B_A* for various Q values between 2.5 and 4 decreased with increasing Al_2O_3 content.
ii. The large range of B_A* values for Q = 4; these B_A values decrease with increasing Al_2O_3 content *ie.* increase in f_{as} (defined in Equation 10).

$$f_{as} = X_{Al_2O_3}/(X_{Al_2O_3} + X_{SiO_2}) \quad (10)$$

The B_A* values at Q = 4 were examined and it was observed that:

i. both ln $\eta_{1900\,K}$ and B_A* decrease with increasing values of f_{as} (defined in Equation 10) as shown in Figures 10 c and e, respectively.
ii. Values of $\Delta \ln \eta_{1900\,K,\,Q=4} = (\ln \eta_{1900\,K,\,Q=4})_{MO^-} - (\ln \eta_{1900\,K,\,Q=4})_{CaO}$ and $\Delta B_A{}^*{}_{Q=4}$ increased with increasing cation size $((r_M/r_{Ca})^3)$ (Figures 10 d and f, respectively).

Thus the introduction of Al_2O_3 into the network results in some change in property values (*ie.* the reduction of both the activation energy and the viscosity) in the region Q = 3 to 4 ie. where the network is well-developed; this may be related to fact that Al-O bond length is smaller than that of the Si-O bond.

Fe_2O_3 and Cr_2O_3 might be expected to behave similarly to Al_2O_3, however, from an analysis of viscosity data it would appear that Fe_2O_3 acts both as a network-breaker (nb) and a network-former (nf). The fraction of the Fe_2O_3 acting as a network breaker ($f_{nb} = f_{nb}/(f_{nb} + f_{nf})$) was ca. 0.6 with f_{nb} increasing with increasing SiO_2 content [8]. A similar analysis of viscosity data indicated that Cr_2O_3 appeared to act as a network-former but Cr_2O_3 did act partially as a network-breaker when Al_2O_3 was present in the slag.

It might be anticipated that TiO_2 would behave like SiO_2 and act largely as a network-former. However, TiO_2 additions were found to reduce viscosities

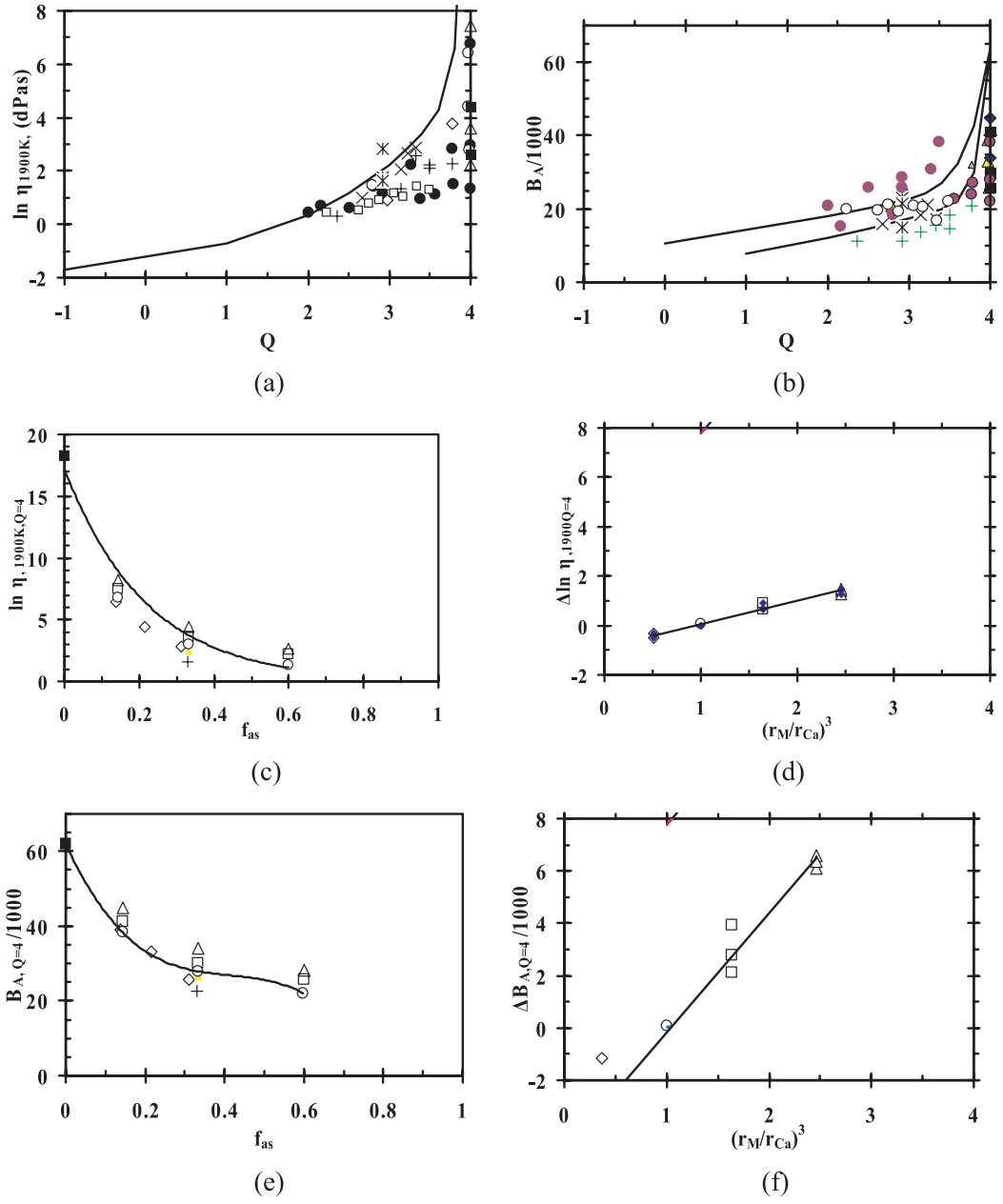

Fig. 10: Values of (a) ln $\eta_{1900\,K}$; ● = CAS; ○ = MAS; ■ = BAS; Δ = SrAS; ◊ = MnAS; + = LAS; x = NAS; * = KAS; □ = CMAS curve = silicates and (b) B_A as functions of Q for both MO and M_2O-SiO_2 systems ● = CAS; ♦ = BAS; ■ = SrAS; Δ = MAS; Δ = MnAS; + = LAS; x = NAS; * = KAS; ○ = CMAS; ■ = SiO_2; +, * and x pertain to lower curve all other symbols to upper curve. (c) ln $\eta_{1900\,K,\,Q=4}$ as a function of fraction Al_2O_3 (f_{as}) Δ = BAS; □ = SrAS; O = CAS; ◊ = MAS; + = MnAS (curve) (d) Δ ln $\eta_{1900\,K,\,Q=4}$ as a function of cation ratio $(r_M/r_{Ca})^3$; Δ ln $\eta_{1900\,K,\,Q=4} = 0.94(r_M/r_{Ca})^3$; (e) $B^*_{A,\,Q=4}$ as function of fas (f); $\Delta B^*_{A,\,Q=4}$ as a function of ratio of cation size $(r_M/r_{Ca})^3$($\Delta B^*_{A,\,Q=4} = -4.762 + 4.57(r_M/r_{Ca})^3$).

[10–13], this suggests that TiO_2 is acting as a *network-breaker*.

Recent work [14–16] indicates that when fluorides are added to a slag, the F^- ions bond with Ca^{2+} ions and form CaF_2 and a slag (denoted here as "*remaining slag*"). However, CaF_2 also causes large reductions in T_{liq} and this may affect the viscosities.

4.4 Density and thermal expansion

4.4.1 Density

Liquid

It has been shown [19] that the densities (ρ) of some slag systems can be satisfactorily described in terms of par-

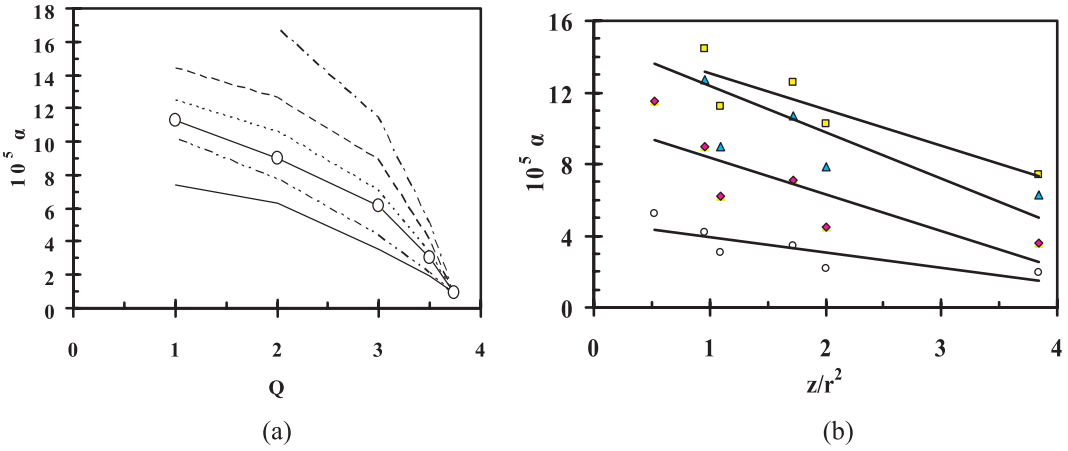

Fig. 11: Thermal expansion coefficient (α) values for liquid MO- and M_2O-SiO_2 slags (after Bockris et al. [46, 47]) as a function of (a) the parameter Q, from the bottom; solid line = MgO; CaO; BaO(o); Li_2O; Na_2O and K_2O, and (b) (z/r^2) *ie*. a measure of the M-O bond strength; ○ = Q = 3.5; ♦ = Q = 3; ▲ = Q = 2; ■ = Q = 1 lines are "best fit" trend lines of data.

tial molar volumes, V, (Equations 11 and 12) where M = molecular weight and subscripts 1, 2, 3 represent different slag components eg. CaO *etc*.

$$V = \Sigma X_1 V_1 + X_2 V_2 + X_2 V_2 + \cdots \quad (11)$$

$$V\rho = M \quad (12)$$

However, in silicate systems it was found that the formation of a network structure resulted in an apparent increase in density (or decrease in molar volume) with increasing SiO_2 content (or Q) [19]; thus the molar volume of SiO_2 is not a constant value but can be represented as a function of X_{SiO_2}. In alumino-silicates, the addition of Al_2O_3 to the silicates results in an apparent reduction in the density (*ie*. increase in molar volume) which can be represented by a polynomial equation. These deviations in molar volume reflect the changes in bonding resulting from the polymerisation of the silicate units and in an alternative approach the molar volume changes were correlated with the enthalpy of mixing [41] for the silicate system.

Solid and supercooled liquid

The density of the crystalline phase is higher than that of the glass because of the tighter packing. The densities at ambient temperature can be calculated in a similar manner to that of the solids (*ie*. using Equations 11 and 12 but with different values for V). Fluegel et al. [20] noted that M_2O additions tended to increase the densities of glasses at temperatures below T_g but reduced the density above T_g (*ie*. in supercooled phase). It would appear that increased expansion at higher temperatures with M_2O additions (Figure 11a) offsets the increases in density derived from the additions.

4.4.2 Thermal expansion

Liquids

Thermal expansion in slags results from the asymmetry of the thermal vibrations produced when a slag is heated. These asymmetric vibrations are affected by (i) the chemical bonding in the slag and (ii) the thermal history of the specimen (*ie*. the cooling rate in formation). Thermal expansion coefficient is usually expressed as either the volume expansion coefficient ($\beta_{T^*} = (V_T - V_{ref})/V_{ref}(T - T_{ref})$) or as the linear expansion coefficient ($\alpha_{T^*} = (L_T - L_{ref})/L_{ref}(T - T_{ref})$) where V and L are the volume and length of the sample and the subscript ref refers to the reference temperature (usually 293 K) and $T^* = 0.5\,(T + T_{ref})$.

The thermal expansion of pure SiO_2 is very low because of the 3-dim. silicate network and resultant symmetry of thermal vibrations but thermal expansion in liquid slags increases as cations are added (ie. decreasing Q); this can be seen in Figure 11a [18]. The hierarchy in the α values shown in Figure 11a ($K_2O > Na_2O > Li_2O > BaO > CaO > MgO$) is approximately that of the MO-bond strengths (as represented by z/r^2) and the plot of α vs z/r^2) is shown in Figure 11b [34]. Thus the thermal expansion in liquid slags can be expressed in terms of Q and (z/r^2).

Solid and supercooled phase

The thermal expansion coefficient (α) for the solid, glass shows the same trend as the liquid, namely, that α

decreases as Q increases and MO-bond strength increases [48]. It has also been reported that α decreases (i) as Al_2O_3, ZrO_2 and TiO_2 levels increase and (ii) with the combination of Na and Ca due to a tightening of the silicate network. There is marked increase in α above T_g ($\alpha_{>Tg} \approx 3\alpha_{<Tg}$) and this causes a change in slope of the density-temperature curve (Figure 4b). It should be noted that additions of K_2O and Na_2O to slags tend to increase the room temperature density (ρ_{298}) but the higher thermal expansion of these slags (see Figure 11a) can result in a decrease in the densities for temperatures in the supercooled region [49].

4.5 Electrical conductivity (κ) and resistivity (R)

The electrical conductivity (κ) is the ability to transport electrons (provided by the cations) under the influence of an applied electrical field. The electrical resistivity (R) is the reciprocal of the conductivity ($R = 1/\kappa$).

4.5.1 Factors affecting electrical resistivity (R)/conductivity (κ)

Database: liquid [50–56] *scl* [33].

The specific electrical conductivity (κ) is the conductivity of a 1 metre cube of the sample and is given by the relation:

$$\kappa = F\Sigma czu \quad (13)$$

where F = Faraday constant, c, z and u are the concentration, charge and mobility of the ionic species.

It can be seen from Equation 13 that the conductivity of liquid slags will increase with increasing cation concentration. The mobility of the cations will be restricted by both the polymerised silicate network and the size of the cations (since smaller cations are more capable of squirming through the gaps in the silicate network). Several workers have equated the resistance to cation movement to the resistance to viscous flow and have correlated electrical resistivity with viscosity [57, 58].

Temperature

The temperature dependencies of the electrical conductivity (κ) and resistivity (R) for a liquid slag are usually represented in the form of an Arrhenius equation:

$$\kappa = A_\kappa \exp(-B_\kappa/T) \quad (14)$$

$$R = A_R \exp(B_R/T) \quad (15)$$

where A_κ = constant; $B_\kappa = (E_\kappa/R^*)$, E_κ = Activation energy and R^* = Gas constant = 8.314 JK^{-1} mol^{-1} and T is in K.

Recent work [34] has shown that the electrical resistivity for the supercooled liquid-correlated exactly with viscosity values represented by a VFT equation (denoted bt subscript V). Thus the temperature dependence of electrical resistivity can be represented by Equation 16.

$$\ln R = A_{R,V} + B_{R,V}/(T - T_o) \quad (16)$$

The T_{liq} effect

It was found in Section 4.3.1. that the experimental scatter in the viscosity data was much smaller for a specific, reference temperature than that at T_{liq} (see Figure 9). Since the resistance to cation movement has been represented by the viscosity [34], the electrical resistance data for T_{liq} and 1900 K are compared (Figures 12 a and b, respectively, for M_2O-silicates and c and d, respectively, for MO-silicates) to see if "*the T_{liq} effect*" also influenced the electrical resistivity data; it can be seen that the scatter is much reduced using a reference temperature of 1900 K.

Effect of silicate structure

It can be seen from Figures 12 b and d that $\ln R_{1900\ K}$ increases with increasing Q and that the relationship exhibits the same "*double exponential*" form as that between $\ln \eta_{1900\ K}$ and Q. It can be seen from Figure 13 that the activation energy term, $B_{A,R}$ also increases with increasing Q but the $B_{A,R}$ values are much greater for the MO-silicates than for M_2O-silicates.

Effect of cation size

Inspection of Figure 12d indicates that the scatter in $\ln R_{1900\ K}$ values (Figures 11(d)) is not random since the larger cations (*eg.* K^+, Ba^{2+}) tend to have higher R values; the scatter shows the magnitude of the effect of cation size on $\ln R_{1900\ K}$ values. This finding is consistent with the view that smaller cations can pass through the silicate network more easily which leads to increasing conductivity (and decreasing R) as cation size increases. Suginohara et al. [55] reported the following hierarchies for

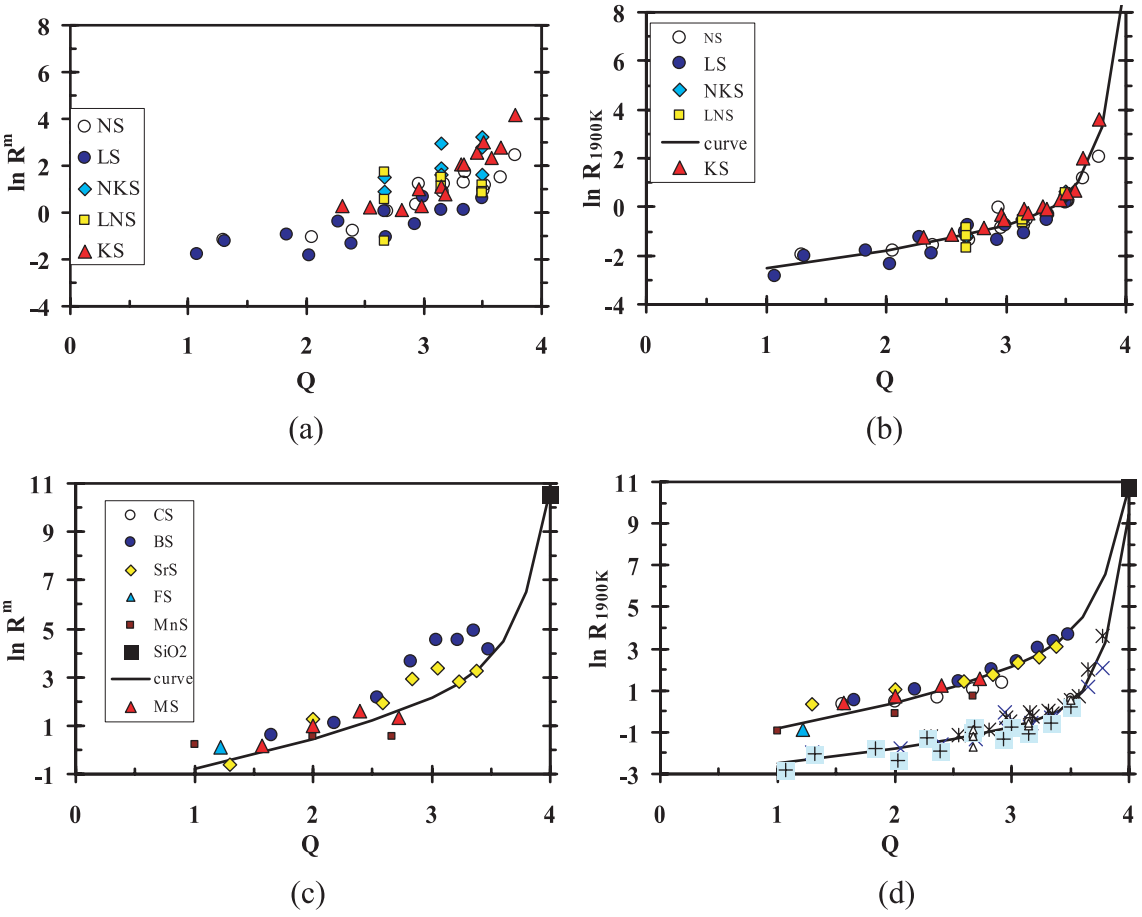

Fig. 12: Values of ln R^m and ln $R_{1900\,K}$ as functions of Q (a) ln R^m for M_2O-SiO_2 systems (b) ln $R_{1900\,K}$ for M_2O-SiO_2 systems (c) ln R^m for MO-SiO_2 systems (d) ln $R_{1900\,K}$ for MO-SiO_2 systems O = CAS; Δ = MS; ■ = MnS; ● = BS; ◊ = SrS; + = LS; x = NS; * = KS; MO-upper curve ln $R_{1900\,K}$ = −4.367 + 2.674 exp(Q/3.428) + 3.5 × 10^{-7} exp(Q/0.239) and M_2O-lower curve ln $R_{1900\,K}$ = −4.777 + 1.702 exp(Q/3.524) + 3.851 × 10^{-9} exp(Q/0.1855).

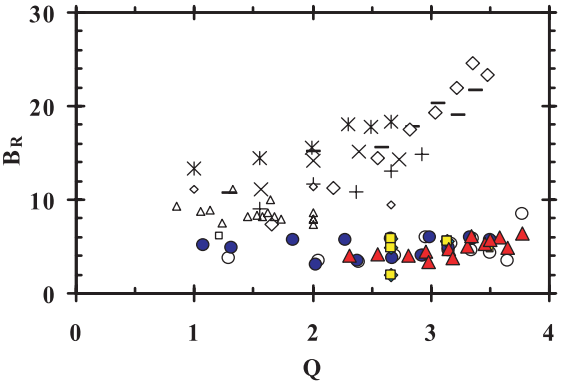

Fig. 13: The activation energy term, $B_{A,R}$ as functions of Q (a); For silicate systems; ○ = CNS; ● = LS; ▲ = KS; ♦ = NKS; □ = LNS; ● = LNS; + = CS; x = MS; – = SrS; ◊ = BS; □ = FS; ◊ = MnS; △ = MFS; * = CMS.

resistivities when different oxides were added to a PbO-SiO_2 slag; $R_{K_2O} > R_{Na_2O} > R_{Li_2O}$. This is in good agreement with the trend shown in Figure 12d but they also found $R_{MgO} > R_{CaO} > R_{BaO}$ which is the reverse of the trend shown Figure 12d.

The resistivities of the data for supercooled phase at specific temperatures were in the hierarchy $R_{K_2O} > R_{Na_2O} > R_{Li_2O}$ [34].

It can be seen from Figure 13 that values for the activation energy parameter, $B_{A,R}$ for the MO-silicates show considerable scatter. It can also be seen that values for the larger cations (eg. Ba^{2+} (◊) and Sr^{2+} (–) tend to lie above those for Ca^{2+} (+) and Mg^{2+} (x). The correction to ln $R_{1900\,K}$ for the MO-silicates approximates to ($\Delta \ln R_{1900\,K} \approx 0.5X_M(r_M/r_{Ca})^3$) and $\Delta B^*_{A,R} \approx 1.5X_M(r_M/r_{Ca})^3$.

It can also be seen that $B_{A,R}$ values for M_2O-silicates are (i) much lower and (ii) the bounds of scatter are much smaller than those for MO-silicates. Furthermore, there is no obvious trend of increasing $B_{A,R}$ values with increasing cation size for M_2O-silicates.

The difference in ln R_{1900} and B_R data (shown in Figures 12b and 13 a, respectively) for Na_2O- and CaO-silicates

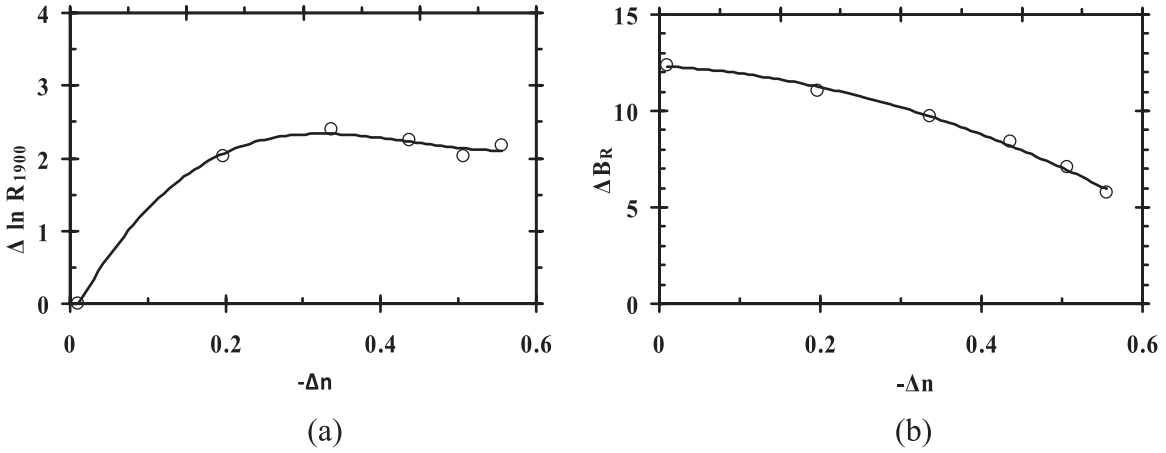

Fig. 14: The effect of $-\Delta n = n_{MO} - n_{M_2O}$ on (a) $\Delta \ln_{R1900} = (\ln_{R1900\ MO} - \ln_{R1900\ M_2O})$ curve $\{\Delta \ln R_{1900}\} = -0.207 + 19.56(\Delta n) - 47.94(\Delta n)^2 + 36.43(\Delta n)^3\}$ and (b) $B_{R1900} = (B_{R1900,\ MO} - B_{R1900,\ M_2O})$ line $\{\Delta B_{R1900} = 12.32 - 2.085(\Delta n) - 16.92(\Delta n)^2\}$.

(which have similar cation sizes) are plotted against the difference in n for the two systems in Figure 14. It can be seen that the change in available cations has significant effects on both $\ln R_{1900}$ and B_R.

Effect of number of available cations

For equivalent compositions (*ie*. identical X_{SiO_2}) there are twice as many cations in M_2O-SiO_2 systems as there are in MO-SiO_2 systems. Thus, the number of available cations (n) can be calculated using Equation 17

$$n = 2\Sigma X_{M_2O} + \Sigma X_{MO} \quad (17)$$

It can be seen from Equation 17 that the replacement of MO by M_2O in silicates will result in a higher conductivity (and lower R). This effect can be clearly seen in Figure 12(d) where the gap between the two curves shows the effect of the greater number of available cations for the M_2O-SiO_2 systems. This gap can be also be seen in Figure 15a where the Na^+ and Ca^{2+} ions have similar sizes and thus the gap reflects the differences in n. The low and relatively flat values of $B_{A,R}$ as a function of Q for M_2O-SiO_2 systems suggests that $B_{A,R}$ is more affected by n than by Q for the slags studied.

Fluegel [33] has reported recommended resistivity data for the *supercooled phase* of Na_2O-CaO-SiO_2 and Na_2O-SiO_2 slags at 1273, 1473 and 1673 K. These data allow one to determine the effect of a change in the number of the available cations (Δn) [33]. The effect of Δn on $\Delta R_{1473\ K}$ can be clearly seen in Figure 15c.

The $B_{A,R}$ values for M_2O-SiO_2 and MO-SiO_2 systems shown in Figure 13 show a large gap between the two sets of data; this gap is largest at high Q values (*ie*. at low cation concentrations and remembering $2n_{Ca^{2+}} = n_{Na^+}$). This suggests that values of the activation energy parameter, $B_{A,R}$ are dependent upon both the polymerisation of the silicate network and the number of available cations, n.

4.5.2 Effects of Al_2O_3, Fe_2O_3, Cr_2O_3, TiO_2, and CaF_2

The effect of incorporating Al_2O_3 into the silicate network is complicated since:

i. It simultaneously decreases the number of available cations (n) and increases Q (because some of the cations must carry out charge-balancing duties); both of these effects result in an *increase* in resistivity.
ii. It results in a decrease in resistance to viscous flow in the region Q = 3 to 4 (as seen in the viscosity, Figures 10a and b) which would tend to *decrease* both $\ln R_{1900\ K}$ and $B_{A,R}$.

Thus these two effects work against each other; for $\ln R_{1900\ K}$ it would appear that the latter effect is more important but for $B_{A,R}$ the effect of n is more important.

In slags containing two or more cations, the resistivity will be affected by which cations carry out the charge-balancing duties. It has been suggested that charge-balancing is carried out by (i) the largest cations [18] (ii) by those with lowest M-O bond strength [59] (*ie*. lowest z/r^2). Here we have assumed that the charge-

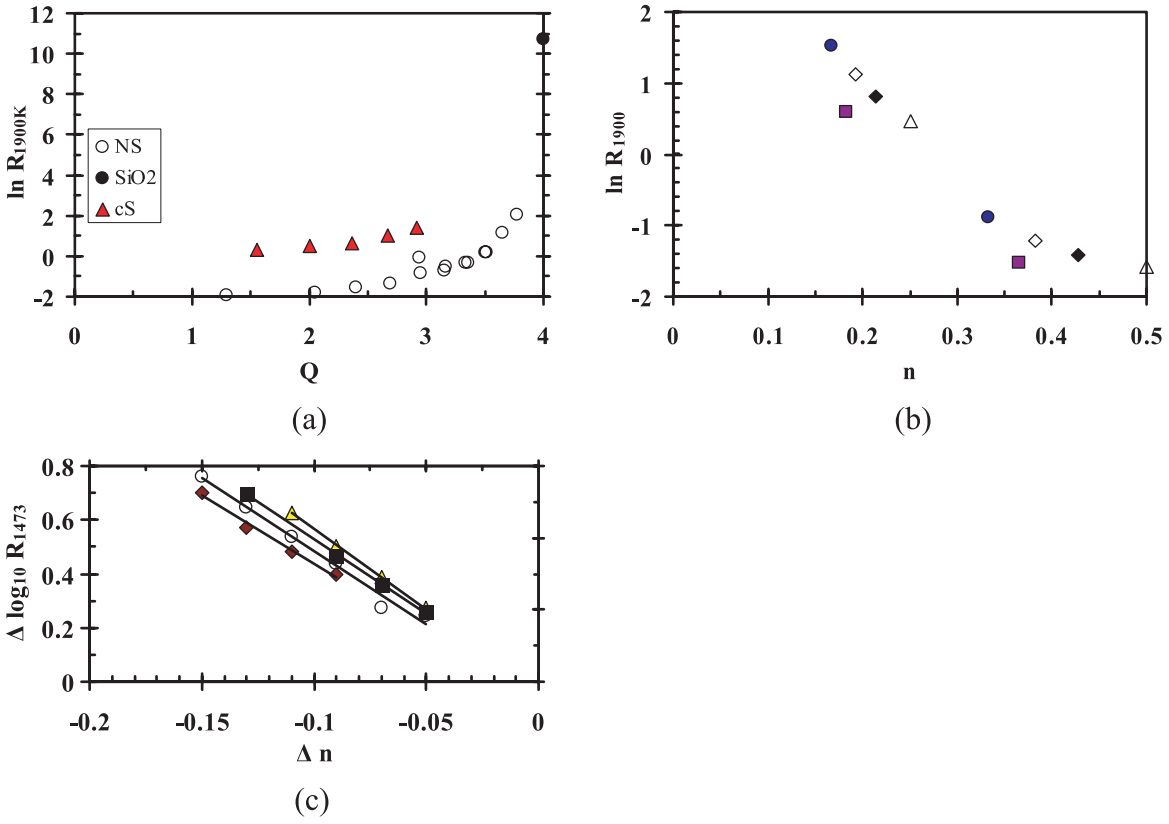

Fig. 15: Values for *scl* of (a) ln $R_{1900\,K}$ as a function of n for CaO-SiO_2 (▲) and Na_2O-SiO_2 (O) systems showing the effect of the number of available cations (n) (b) the data for Na_2O-SiO_2 and CaO-SiO_2 as functions of n and (c) Change in resistivity (Δ_n $\log_{10}$ R_{1473}) of Na_2O-CaO-SiO_2 and Na_2O-SiO_2 slags as a function of the change in the number of cations (Δn) for groups with identical Q values ♦, Q = 2.97; O; Q = 3.14; ■, Q = 3.22; Δ, Q = 3.30.

balancing is statistical based on the concentrations of cations present. Thus in alumino-silicates n can be calculated by

$$n = (1 - f_{cb})\{2\Sigma X_{M_2O} + \Sigma X_{MO}\} \quad (18)$$

where f_{cb} is the fraction of cations on charge-balancing duties ($1 - f_{cb} = (\Sigma X_{M_2O} + \Sigma X_{MO} - X_{Al_2O_3})/(\Sigma X_{M_2O} + \Sigma X_{MO})$).

It can be seen from Figure 16 that:

i. Values for ln $R_{1900\,K}$ depart from the silicate curve around Q = 3 and subsequently, adopt lower values than those given by the CaO-SiO_2 curve.
ii. the parameter $B_{A,R}$ is significantly higher than the CaO-SiO_2 curve which is consistent with the fact that $B_{A,R}$ increases as the number of available cations (n) decreases.

TiO_2 additions have little effect on the ln $R_{1550\,K}$ and $B_{A,R}$ up to $X_{TiO_2} = 0.1$ but any further additions result in increasing R and $B_{A,R}$ values [52].

4.5.3 Equation for electrical resistivity of liquid and supercooled phases

In summary, ln R_{Tref} can be expressed as (i) a double exponential equation involving Q (ii) a smaller term involving cation size and (iii) and a third term involving n. It should be noted that initially the third term, involving (1/n) was used but did not provide a good fit and a much better fit was obtained using an equation of the form shown in Equation 19 where c and t are constants. Similarly, $B_{A,R}$ = can be expressed by Equation 20 but it will be necessary to derive separate relations for MO- and M_2O-silicates.

$$\ln R = y + c_1 \exp(Q/t_1) + c_2 \exp(Q/t_1) - c_3 n + c_4(r^3) \quad (19)$$

$$B_{A,R} = y + c_1 \exp(Q/t_1) + c_2 \exp(Q/t_1) - c_3 n + c_4(r^3) \quad (20)$$

In the case of alumino-silicates, the ln R_{Tref} is derived from the Equation 19 but a correction based on f_{as} must be applied. A similar procedure involving Equation 20 can be applied to calculate $B_{A,R}$.

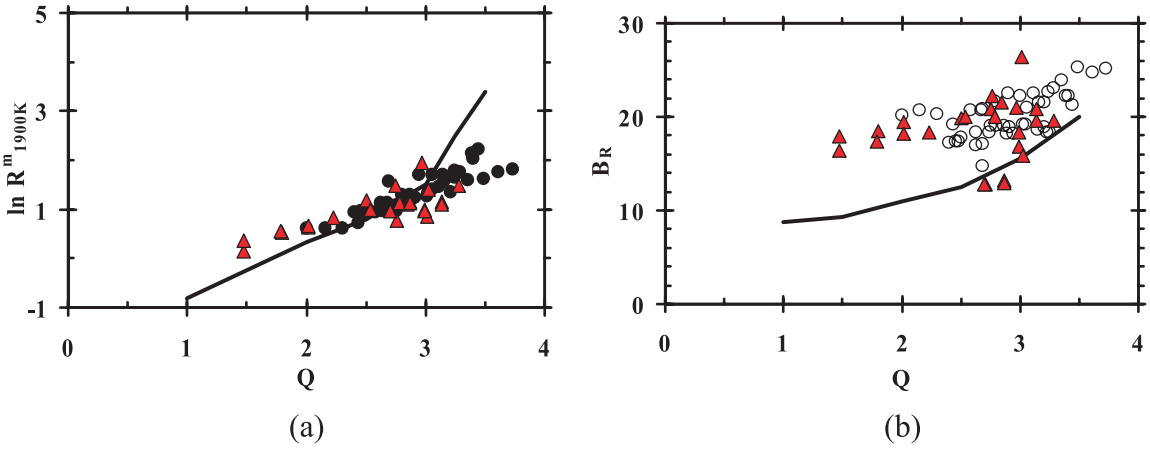

Fig. 16: Values of ln $R_{1900\,K}$ and (b) $B_{A,R}$ as functions of Q; curve = curve for silicates and ● = CAS, ▲ = CMAS, ■ = SiO_2 and (b) alumino-silicates; curve = CS; ○ = CAS; ▲ = CMSA.

4.6 Themal conductivity (k)

When slags are heated the molecules become agitated and vibrate and heat is conducted by *phonons ie. lattice waves*.

4.6.1 Measurement problems

Thermal conductivity measurements are subject to two severe measurement problems. The first problem involves the elimination of contributions from *convection* to the thermal conductivity of the liquid. This problem is minimised by using transient techniques, namely, the transient hot wire (THW) method or the laser pulse (LP) method [60]. The second problem arises from contributions from *radiation conductivity* (k_R) which involves a process of absorption of IR radiation by the sample and subsequent re-emission. Radiation conductivity increases with increasing sample thickness until a certain critical thickness is attained (whereupon the sample is said to be *optically thick*). The magnitude of k_R can be significantly decreased by (i) *absorption* if transition metal oxides (eg. FeO, CrO) are present and (ii) by *scattering* if crystallites and grain boundaries in slag sample. The apparent thermal conductivity (k_{app}) contains contributions from both the lattice thermal conductivity (k_c) and from radiation conductivity, k_R; the contributions from k_R increase significantly at higher temperatures (>800 K). The THW measurements are preferred because LP values tend to have larger contributions from k_R due the larger emitting surface which has a surface area 10× greater than that in THW studies. For this reason only data obtained by the THW method have been adopted here.

$$k_{app} = k_c + k_R \tag{21}$$

4.6.2 Factors affecting thermal conductivity

Database- [61–68]

Temperature

The temperature dependence shown in Figure 17 is typical of many slags.

The curve shown in Figure 17a can be divided into 3 regions:

i. a region (between 298 K and T_{crit}) for the solid where k-T is reasonably steady.
ii. A region (between T_{crit} and T_{liq}) in which there is a dramatic drop in thermal conductivity.
iii. The liquid region above T_{liq} in which the values of k tend to be low and the experimental scatter is about ±0.05 $Wm^{-1}\,K^{-1}$.

Thus the curve can be approximately defined by three points, namely, k_{298}, k_{Tcrit} and k_{Tliq} (= k^m). It was originally proposed that sharp drop in k occurred at T_g when the glass transformed into a supercooled liquid [69]. However, it has been shown [34] that T_{crit} occurred when the viscosity of the *scl* reached a value of 10^6 dPas (Figure 16 b) which lies between the softening temperature (where a sample collapses under its own weight) and the flow temperature. Consequently, it would appear that the thermal conductivity of the solid and *scl* is related to the *rigidity* of the silicate network. Thus anything which improves the

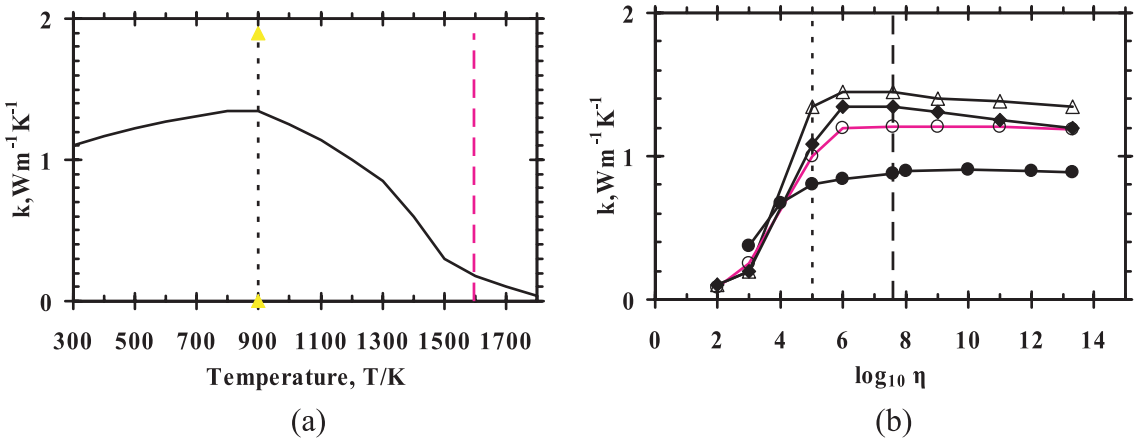

Fig. 17: Themal conductivity as a function of (a) temperature for $0.1Na_2O$-0.4CaO-$0.5SiO_2$ [63] – – = T_{liq}; •••• = T_{crit} and (b) $\log_{10}$ viscosity [35] for Δ = NS_4; ♦ = NS_3; ○ = NS_2, ● = KS_2 in the supercooled phase; – – – = T_{soft}; ••••• = T_{flow} [61, 66].

rigidity of the silicate network would be expected to increase the thermal conductivity of the solid and *scl*, *eg*.

i. increasing polymerisation of the silicate network (increasing Q)
ii. M-O bond strength might be expected to increase k (slags containing CaO and Li_2O appear to have high k_{298} and k_{Tcrit} values)
iii. The combination of Na_2O and CaO tightened the network and thereby reduced the thermal expansion of solid glasses [48] and that appears to be the case also for k in the range (298 K-T_{crit})

The following equation has been derived to estimate T_{crit} [34] from a "*best-fit*" of composition data and calculated temperatures where $\eta = 10^6$ dPas using the model due to Fluegel [35].

$$\begin{aligned} T_{crit}(K) = 2158.5 &- 914X_{SiO_2} - 1109X_{CaO} - 5.67X_{Al_2O_3} \\ &- 1820X_{Na_2O} - 2838X_{Li_2O} - 1835X_{K_2O} - 855X_{MgO} \\ &- 1323X_{SrO} - 1450X_{BaO} - 1500X_{CaF_2} - 1501X_{TiO_2} \\ &- 47.6X_{ZrO_2} - 2159X_{Fe_2O_3} \end{aligned} \quad (22)$$

Effect of silicate structure

Liquid slags

The thermal conductivities of liquid slags have been found to increase with increasing SiO_2 content or polymerisation (*ie*. Q) [18, 64, 66]. The values of the thermal conductivity at the liquidus temperature (k^m) and at 1773 K ($k_{1773\,K}$) are plotted in Figure 17a and b, respectively. All the curves of k versus Q in Figure 18 show the same, exponential form as the viscosity. The thermal conductivity appears to be following the viscosity. This view is supported by the linear relation found between ln k and ln η [66] and the use of an Arrhenius equation for the temperature dependence of liquid slags [67]. Since it is the electrical resistivity which follows viscosity, it is interesting to note that the thermal conductivity follows the electrical resistivity and thus k is inversely dependent on the electrical conductivity.

It is difficult to derive reliable $B_{A,R}$ values because of the limited temperature range of measurements for the liquid and the experimental uncertainties of the measurements. It was found that the $B_{A,R}$ values reported by Kang and Morita were about $0.75B_{A,R}$ values for the viscosity.

Liquidus temperature effect

The T_{liq} effect was investigated; it can be seen from Figures 18a and b (or c and d) that using a reference temperature of 1773 K does not help to reduce the scatter in the experimental results. Any benefits of comparing values of $k_{1773\,K}$ are offset by the facts that k values tend to be low and experimental uncertainties are of a similar magnitude to k itself, for slags with Q < 3.

Cation effects

It was anticipated that the M-O bond strengths would affect k. The deviations from the various curves shown in Figure 18 were plotted against (z/r^2) and ($X\ z/r^2$) but no trend could be identified.

Solid and Supercooled phases

Solid slags are either crystalline or glass phases or a mixture of the two. Thermal conductivities at ambient

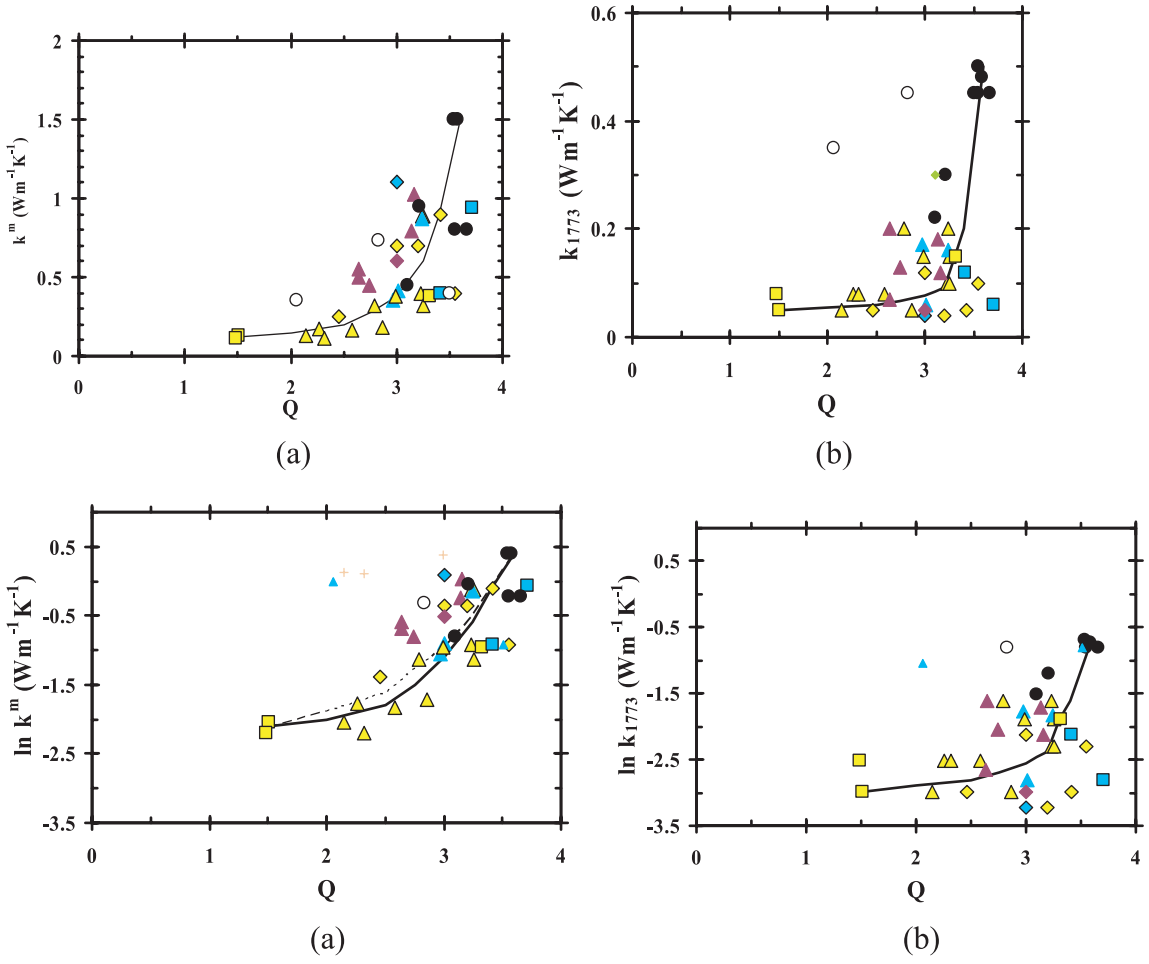

Fig. 18: Thermal conductivity of liquid slags as a function of Q for (a) k^m (b) k_{1773} (c) ln k^m and (d) ln k^m; ♦ = LS; ◊ = NS; ♦ = KS; O = CS; Δ = CNS; ▲ = CLS; ▲ = CKS; = CAS; ● = CAS; ■ = LAS; □ = NAS; ***DatabthcondAK46***

temperatures of crystalline slags are 1.5–2.5 times those of glassy slags due to the higher packing densities in crystalline phases [68]. Thus the presence of any crystalline phase in the sample will tend to give a higher thermal conductivity.

An examination of thermal conductivity data for M_2O-CaO-SiO_2 and M_2O-SiO_2 systems [63–66] indicated that k_{298} and k_{Tcrit} values increased as:

i. the SiO_2 content (X_{SiO_2}) increased
ii. M_2O was increasingly replaced by CaO
iii. As Li_2O content increased ($k_{Li_2O} > k_{Na_2O} > k_{K_2O}$)

This was interpreted as indicating k_{298} and k_{Tcrit} increased as (i) Q increased and (ii) MO-bond strength (z/r^2) increased.

There are few data for the temperature dependencies of the thermal conductivities of slags. The $B_{A,k}$ values reported by Kang and Morita [67] approximate to $B_{A,k} \approx 0.75B_{A,\eta}$.

4.7 Surface tension (γ)

Surface tension (γ) differs from all the other properties mentioned above, in that it is a *surface property* and not a *bulk property*. The surface layers of liquids tend to have high concentrations of constituents with low surface tension (known as "*surfactants*") in their surface, or interface, layer; SiO_2 has a reasonably-low surface tension (*cf.* MgO, CaO etc.) but typical surfactants in slags are B_2O_3, K_2O and CaF_2. Surface tensions of slags (such as CaO-SiO_2 system) with no surfactants present can be estimated from partial molar values ($\gamma = \Sigma X_{CaO}\gamma_{CaO} + X_{SiO_2}\gamma_{SiO_2} +$) [70, 71]. However, the presence of surfactants tends to cause significant reduction of the overall surface tension.

It can be seen from Table 2 that the surface tensions (i) of MO-silicates are significantly higher than those for M_2O-silicates and (ii) and for M_2O-silicates surface tensions decrease as MO-bond strengths (or z/r^2 values) decrease. Since the surface tension of SiO_2 is low *cf* CaO or

	SiO_2	CaO	BaO	SrO	MgO	Al_2O_3	MgO	FeO	NiO	MnO	CrO	Na_2O	K_2O	TiO_2	ZrO_2	Cr_2O_3	Fe_2O_3	CaF_2	B_2O_3
γ	260	625	560	600	635	655	635	645	645	645	360	295	160	360	400	800	300	290	110

Table 2: Surface tensions (mNm^{-1}) of pure slag components at 1773 K

MgO, then surface tensions tend to decrease as the SiO_2 content (or Q) of the slag increases. The surface concentration will also be dependent on the activity coefficient of silica ($f^*_{SiO_2}$); in M^nO-SiO_2 melts, $f^*_{SiO_2}$ is promoted by low values of the M-O bond strength (or low values of (z/r^2) for the oxide). Consequently, slag constituents like K_2O, possess both a low surface tension and will also tend to increase the SiO_2 concentration in the surface layer; both will lead to a low γ value.

When the concentration of surfactants at the free surface exceeds a certain critical value the temperature dependence (dγ/dT) tends to change from a negative value to a positive value. Since silica is a mild surfactant in molten silicates, this critical point is reached when SiO_2 mass% exceeded 50% [72, 73]. It might be expected that for M^nO-SiO_2 melts, systems with high f_{SiO_2} values (*eg.* $K_2O > Na_2O > Li_2O > BaO$) would assist positive (dγ/dT) values.

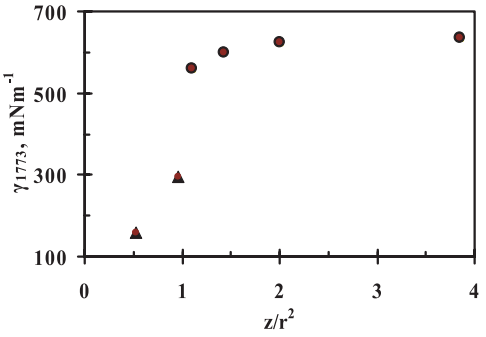

Fig. 19: Surface tension of slag constituents, MO (●) and M_2O (▲) oxides at 1773 K as a function of bond strength (ie. (z/r^2)).

5 Discussion

The factors affecting individual thermo-physical properties are summarised in Table 3. It can be seen that:

i. the ***strength of the M-O bond*** affects the magnitude of T_{liq}, the chemical activity coefficient of SiO_2 and the entropy of fusion and probably influences surface tension and the thermal conductivity (through its effect on the rigidity of the silicate lattice).
ii. It is not known for certain whether ***bridging of two chains*** by M^{2+} affects the viscosity and possibly electrical resistivity and thermal conductivity values. However, the lower values for the activation energy parameter, B_A found for M_2O-silicates (*cf.* MO-silicates) supports the view that *bridging* affects these properties.
iii. the ***cation size*** certainly affects the electrical resistivity and the viscosity.
iv. the ***number of cations*** has a significant effect on the electrical conductivity.

More work and more data are needed in certain areas *eg.* thermal conductivity measurements and in determining

Property	Factors	Bridging	M-O bond strength	M-O covalence	Cation size	Mixed cation effect	Number of cations
T_{liq} ↑			↑				
$f^*_{SiO_2}$ ↑	Q↑ (z/r^2) ↓		↓				
ΔS^{fus} ↑	Q↓ (z/r^2) ↑		↑				
α, β ↑	Q↓ (z/r^2) ↓		↓	Possibly			
ln η_{Tref} ↑	Q↑ (r^3)				(r^3)		
B_A↑	Q↑	↑					
ln R(= ln κ^{-1})↑	Q↑ n↓ (r^3) ↑	Probably			(r^3) ↑	↑	↑
$B_{A,R}$↑	Q↑ n↓ (r^3) ↑	Probably					
k↑	Rigidity↑ Q↑ (z/r^2) ↑?	Probably	↑?	Possibly		Possibly	
γ↑	X_{SiO_2}↓ Q↓		Probably				

Table 3: Summary of the factors affecting various properties of slags; ↑ indicates an increase in property obtained, for instance, by a decrease (↓) in M-O bond strength; $f^*_{SiO_2}$ = activity coefficient of SiO_2.

the effects of components like Cr_2O_3 on both the slag structure and the various properties.

Conclusions

1. Some procedures used in modelling property values appear to be flawed or of limited use for instance:
   i. It is shown here the scatter in experimental data at a reference temperature for viscosity and electrical resistivity is significantly smaller than that at the liquidus temperature
   ii. the relation between the Arrhenius parameters ln A and B is a non-linear function.
2. The principal factors affecting the following properties are:
   Viscosity – the degree of polymerisation (Q) and a smaller effect involving cation size
   Electrical resistivity – involves (i) Q (ii) the size of the cations and (iii) the number of available cations
   Thermal expansion involves (i) Q and (ii) the M-O bond strength (which can be represented by z/r^2)
   Thermal conductivity values appear to be linked to the *rigidity* of the silicate network and it is thought that these involve (i) Q and (ii) M-O bond strength but more work is needed to establish the factors influencing the thermal conductivity of solid and liquid slags.
3. The absorption of Al^{3+} ions into silicate (Si^{4+}) chains does affect the physical properties especially where the silicate network is well-developed (*ie*. Q = 3 to 4).
4. Analysis of viscosity data indicate that Fe_2O_3 acts as both a network breaker and network former and that Cr_2O_3 acts predominantly as a network former and only works as a partial network breaker when Al_2O_3 is present in reasonable concentrations.

Symbols, abbreviations and units

C_p = Heat capacity ($JK^{-1}\ kg^{-1}$)
f = fraction
f* = activitiy coefficient
H = enthalpy, Jkg^{-1}
k = Thermal conductivity ($Wm^{-1}\ K^{-1}$)
n = number of available cations
Q = Measure of polymerisation of melt (= 4-NBO/T)
R = Electrical resistivity (Ω cm = $10^2\ \Omega$ m)
r = Cation radius (10^{-10} m)
T = temperature, K
T_g = Glass transition temperature, K
T_{liq} = Liquidus temperature, K
V = molar volume ($cm^3\ mol^{-1}$)
X = mole fraction
z = Charge on cations
α,β = linear and volume thermal expansion coefficient (K^{-1})
γ = surface tension (mNm^{-1})
η = Dynamic Viscosity (mPas)
κ = Electrical conductivity ($\Omega^{-1}\ cm^{-1} = 10^{-2}\ \Omega^{-1}\ m^{-1}$)
ρ = Density ($kg\ m^{-3}$)
NBO/T = Non-bridging oxygen/Tetragonal Oxygen
scl = supercooled liquid
% = mass%

Superscripts
m = Value at liquidus temperature

In figure captions the following abbreviations are used for chemical formulae: A = Al_2O_3; B = BaO; C = CaO; F = FeO; K = K_2O; L = Li_2O; M = MgO; Mn = MnO; N = Na_2O; S = SiO_2 and Sr = SrO.

Acknowledgements

The authors thank Prof. M Susa (Tokyo Tech.) and Prof. Seshadri Seetharaman (KTH, Stockholm) for their valuable discussion and comments.

Received: May 20, 2012. Accepted: July 12, 2012.

References

[1] KC Mills and AB Fox: *ISIJ Intl*. **43**, 1479/1486 (2003).
[2] P Ramirez-Lopez, KC Mills, PD Lee and B Santillana: *Metall. Mater. Trans B*. **43B** (1) 109/122 (2012).
[3] P Ramirez-Lopez, KC Mills, PD Lee and B Santillana: *ISIJ Intl*. **50** (12) 1797/1804 (2010).
[4] BO Mysen: *Structure and Properties of silicate melts*, publ Elsevier, Amsterdam (1988).
[5] BO Mysen: *Earth Science Reviews*, **27**, 281/365 (1990).
[6] *Slag Atlas*, publ Stahl u Eisen, VDEh, Dusseldorf (1995).
[7] G Urbain: *Steel Research*, **58**, 111/116 (1987).
[8] KC Mills, L Yuan and Z Li: *Estimation of the thermo-physical properties of slags Part 1 Viscosity* to be published.
[9] T Iida and Y Shiraishi: Chapter 4 Viscosity, *Handbook of Physico-chemical Properties at high temperatures*. edited Y Kawai and Y Shiraishi, publ. ISIJ Special Issue No. 41 Tokyo (1988) pp. 127/144.
[10] A van Bernst and C Delaunois: *Verres Defract* **20**, 435 (1966).
[11] T Nakamura, K Morinaga and T Yanagase: *Nippon Kinzoku Gakkaishi* **41**, 1300 (1977).
[12] S Yagi, K Mizoguchi and Y Suginahara: *Bull. Kyushu Inst. Technol. Sci Technol*., No **40** 33 (1980).

[13] A Shankah: *Studies of high-alumina blast-furnace slags*, PhD thesis, KTH, Stockholm (2007).
[14] Y Sasaki, M Iguchi and M Hino: *ISIJ Intl.* **47**, 346/347 (2007).
[15] Y Sasaki, M Iguchi and M Hino: *ISIJ Intl*. **47**, 638/642 and 1370/1371 (2007).
[16] T Asado, Y Yamada and K Ito: *ISIJ Intl*. **48**, 120/122 (2008).
[17] T Iida, H Sakai, Y Kita and K Murakami: *High Temp. Mater. Processes*, **19**, 153/164 (2000).
[18] KC Mills: *ISIJ Intl.* **33**, 148/156 (1993).
[19] VK Gupta, SP Sinha and B Raj: *Steel India* **21**, 22/29 (1998) 22/29 and **17** (1994) 74/78.
[20] KC Mills and S Sridhar: *Ironmaking and Steelmaking*, **26**, 262/268 (1999).
[21] J Duffy and MD Ingram: *J Non-Cryst. Solids* **21**, 373/410 (1976).
[22] T Nakamura, Y Ueda and JM Toguri: *J Jap. Inst. Metals*, **50** (5) 456/461 (1986).
[23] H Gaye and J Welfinger: *2nd Intl. Symp. Metall. Slags and glasses* held Lake Tahoe, NV edited HA Fine and DR Gaskell publ TMS-AIME Warrendale, PA (1984) 357/275.
[24] Ling Zhang, S Sun and S Jahanshai: *Metall Trans B*, **29B**, 177/186 (1998).
[25] Ling Zhang, S Sun and S Jahanshai: *Metall Trans B*, **29B**, 187/195 (1998).
[26] GH Zhang, KC Chou, G Xue and KC Mills: *Metall. Mater. Trans. B*, **43B**, 64/72 (2012).
[27] GH Zhang, KC Chou, and KC Mills: *ISIJ Intl*. **52**, 355/362 (2012).
[28] GH Zhang and KC Chou: *J Min. Metall. B*, **48**, 1/10 (2012).
[29] GH Zhang and KC Chou: The influence of CaF_2 on viscosity of alumino-silicate melts. Ironmaking and Steelmaking in press (2012).
[30] K Takahashi and A Osaka: *J Ceram. Soc. Jap*. **91**, 359 (1983) and **78**, 329 (1970) cited in ref. 64.
[31] Wikipedia: www.wikipedia.org/wiki/Ionic_radius.
[32] M Nakamoto, A Kiyose, T Tanaka, L Holappa and M Hamalainen: *ISIJ Intl*. **47**, 38/43 (2007).
[33] A Fluegel: *Electrical resistivity of silicate glass melts based on SciGlass Database*. http://glassproperties.com. 2007, p. 21.
[34] KC Mills, L Yuan, Z Li, GH Zhang and KC Chou: *Proceedings of 9th Intl. Conf. Molten slags, fluxes and salts (Molten 12)* held Beijing China May 2012.
[35] A Fluegel: *Glass viscosity calculation based on a global statistical modelling approach*. *J Glass Sci. Technol*. **48**, 13/36 (2007) and Glass Viscosity calculator: see also website http://glassproperties.com/viscosity/.
[36] KC Mills, L Yuan, Z Li and RT Jones: *J South Afr. Inst. Min. Metall*. **111**, 649/658 (2011).
[37] MTDATA web site: www.npl.co.uk/mtdata/.
[38] Factsage web site; www.factsage.com/.
[39] Thermocalc web site; www.thermocalc.com.
[40] G Urbain, Y Bottinga and P Richet: *Geochim. Cosmochim. Acta* **46**, 1061/1072 (1982).
[41] M Persson, PhD Thesis, *Investigations of slag properties and Reactions*. Metallurgical Process Science, KTH, Stockholm (2007).
[42] F Ji: Licentiate Thesis; *Experimental studies of viscosities of some multicomponent sla*gs. Dept. Metallurgy, KTH, Stockholm (1997).
[43] F Shahbazian: Licentiate Thesis *Viscosities of some CaF_2-containing slags*. Dept. Metallurgy, KTH, Stockholm (1998).
[44] L Forsbacka: PhD Thesis. *Experimental study and modelling of viscosity of Cr-containing slags.* Helsinki Univ. Technology. Espoo, Finland (2007).
[45] GH Zhang and KC Chou: *Metall. Mater. Trans. B*, in press, (2012).
[46] J O'M Bockris, JA Kitchener, S Ignatowicz and JW Tomlinson, *Trans. Farad. Soc*. **48**, 75 (1952).
[47] J O'M Bockris, JA MacKenzie and JA Kitchener: *Trans Farad Soc*. **55**, 1734 (1955).
[48] A Fluegel: *Thermal expansion calculation of silicate glasses at 210 °C based on systematic analysis of global databases*. http://glassproperties.com, 2007.
[49] A Fluegel, DA Earl, AK Varshneya and TP Seward III; Density and thermal expansion calculation of silicate glass melts from 1000 to 1400 °C. *Eur. J Glass Sci. & Technol Part B*, **49**, 245/257 (2008).
[50] J O'M Bockris, JA Kitchener, S Ignatowicz and JW Tomlinson: *Trans. Farad. Soc.* **48**, 75/91 (1952).
[51] RE Tickle: *Phys. Chem. Glasses*, **8**, 101/112 (1967).
[52] K Mori: *Tetsu-to-Hagane* **42** (8) 633/638 (2009).
[53] H Keller, K Schwerdtfeger and K Hennessen: *Metall. Mater. Trans B*, **10**, 67/70 (1979).
[54] L Segers, A Fontana and R Winland: *Trans. Inst. Min. Metall. C*, **88**, C53–C56 (1979).
[55] Y Suginohara, T Yanagase and H Ito: *Trans. Japan Inst. Metals*, **3**, 227/233 (1962).
[56] Q Jiao and NJ Themelis: *Metall. Trans B*, **19B**, 133/140 (1988).
[57] M Kato and S Minowa: *Tetsu-to Hagane*. **55**, 260/286 (1969).
[58] GH Zhang and KC Chou: *Metall. Mater. Trans B*, **43B**, 261/264 (2012).
[59] GH Zhang and Kuo-Chih Chou, Viscosity model for aluminosilicate melt, *J. Min. Metall. B*, in press, (2012).
[60] R Gardon: Proc 2nd Intl Thermal Conductivity Conference held Ottawa (1962) 167.
[61] K Nagata and KS Goto: *Proc. 2nd Intl. Conf. On Metallurgical slags and fluxes* held Lake Tahoe, NV, (1984) edited HA Fine and DR Gaskell publ. TMS-AIME, Warrendale, PA 875.
[62] M Susa, S Kubota, M Hayashi and KC Mills*: Ironmaking and Steelmaking*, **28**, 390/395 (2001).
[63] S Ozawa and M Susa: *Ironmaking and Steelmaking*, **32**, 487/493 (2005).
[64] S Ozawa, R Endo and M Susa: *Tetsu-to-Hagane*, **93**, 8/15 (2007).
[65] M Susa, M Watanabe, S Ozawa and R Endo: *Ironmaking and Steelmaking*, **34**, 124/130 (2007).
[66] M Hayashi, H Ishii, M Susa, H Fukuyama and K Nagata: *Phys. Chem. Glasses*, **42**, 6 (2001).
[67] Y Kang and K Morita: *ISIJ Intl.* **46**, 420/426 (2006).
[68] K Nishioka, T Maeda and M Shimizu: *ISIJ Intl.* **46**, 427/433 (2006).
[69] KC Mills: *Proc. 3rd Intl. Conf. on Molten slags and fluxes*, held Glasgow, 1988 publ. Inst of Metals, London 1989, pp. 229/234.
[70] RE Boni and G Derge: *J Metals* **206**, 53 (1956).
[71] KC Mills: *ACS Symposium Series 301, Mineral matter and ash in coal* edited KS Vorres, publ. Amer. Chem. Soc. (1986), pp. 195/214.
[72] K Mukai and T Ishikawa: *Nippon Kinzoku Gakkaishi*, **45** (2) 147 (1981).
[73] TB King: *J Soc. Glass Technol*. **35**, 241 (1951).